International Journal of Climatology

International Journal of Climatology | RMetS

RESEARCH ARTICLE OPEN ACCESS

User-Relevant Climate Indices and Associated Uncertainties From Transient Convection-Permitting Climate Model Projections

Joaquim G. Pinto[1] | Marie Hundhausen[1] | Annabell Weber[1,2] | Regina Kohlhepp[1,3] | Christine Mihalyfi-Dean[1,4] | Janus W. Schipper[1,4] | Hendrik Feldmann[1]

[1]Institute of Meteorology and Climate Research – Troposphere Research (IMKTRO), Karlsruhe Institute of Technology (KIT), Karlsruhe, Germany | [2]Deutsches Zentrum für Luft- Und Raumfahrt (DLR), Institut für Physik der Atmosphäre, Oberpfaffenhofen, Germany | [3]Landesanstalt für Umwelt Baden-Württemberg (LUBW), Karlsruhe, Germany | [4]South German Climate Office, Karlsruhe Institute of Technology (KIT), Karlsruhe, Germany

Correspondence: Joaquim G. Pinto (joaquim.pinto@kit.edu)

Received: 6 June 2025 | **Revised:** 16 December 2025 | **Accepted:** 5 February 2026

Keywords: climate adaptation | climate indices | convection-permitting | COSMO-CLM | extremes | multi-model ensemble | regional climate modelling

ABSTRACT

Ongoing climate change is leading to considerable alterations of the mean climate, the day-to-day weather and their variability. This poses substantial challenges for stakeholders and increases the urgency to develop adequate adaptation and mitigation strategies. In order to represent the local changes in climate across different regions as accurately as possible, and provide useful and usable information for stakeholders, we use an ensemble of convection-permitting climate simulations to quantify the projected changes for user-relevant climate indices for Southern and Central Germany. A wide range of temperature, precipitation, and user-oriented climate indices relevant to various stakeholder applications to address their information requirements are considered. After bias adjustment, the indices are in very good agreement with results using the HYRAS dataset, though small shortcomings remain. Regarding the climate change signal, several different patterns can be identified. For high temperature indices, a significant increase is observed, particularly for very hot days and tropical nights. On the other hand, the number of frost and ice days significantly decreases with global warming. Other indices like hiking days and summer dry days show comparatively small changes. While relative changes are largest for high altitude areas for high temperature indices, their absolute changes are largest for low areas like the Rhine Valley. For high temperature indices, an increase both in mean values and variability is found with global warming. The opposite is true for snow days, ice days and winter service days. We conclude that convection-permitting simulations can be key to provide usable user-relevant climate indices for recent climate conditions and projections for future decades, both considering high spatial resolution and uncertainty estimations. Such a database can thus be extremely useful for the development and implementation of informed adaptation measures to climate change, as discussed in detail for specific examples in Germany.

1 | Introduction

The recent decades have been characterised by a wide range of weather and climate extremes, including heat waves, droughts, extreme floods, and storms (e.g., Schär and Jendritzky 2004; Barriopedro et al. 2011; Mohr et al. 2023). Climate models are a very helpful tool to provide information for past, present, and future climate conditions, and provide realisations of the future development of our weather and climate (Randall et al. 2019; Bordoni et al. 2025). While global climate models

(GCMs) typically lack the required spatial and time scales to analyse regional extremes, downscaling with regional climate models (RCMs) provides a clear added value towards that aim (e.g., Jacob et al. 2014). Over the last decade, a new generation of high-resolution models with a grid spacing under 4 km has been developed (e.g., Prein et al. 2015). These convection-permitting models (CPMs) provide multiple advantages, e.g., in the representation of convective precipitation and extremes in spatial heterogeneous regions like urban or mountainous environments (Prein et al. 2015; Tölle et al. 2018; Lucas-Picher et al. 2021). Ensemble simulations are required to quantify the uncertainties of the climate projections. With this aim, the first CPM ensembles were developed, like for the CORDEX Flagship Pilot Study on Convection for the Alpine area for 10-year time slices (FPSConv; Pichelli et al. 2021; Ban et al. 2021). Recently, first transient CPM ensemble projections were presented (Kendon et al. 2023; Hundhausen et al. 2023). Such CPM ensemble simulations provide the necessary data to analyse climate variability and trends for different global warming levels (GWLs), as used in the most recent IPCC Assessment Report (IPCC 2023; Lee et al. 2015). The GWL concept facilitates the discussion of uncertainties in climate projections, as it allows comparison of climate change signals for GCMs with different climate sensitivity and different emission scenarios. Combined with the application of bias adjustment to account for the systematic error in the model output (e.g., Maraun 2016), they provide an important step towards the usability of climate model data.

Traditionally, climate scientists have focussed their assessment of climate change predictions and projections primarily on basic variables like precipitation, wind, temperature, and sometimes on their extremes (IPCC 2007). While very valuable for the evaluation of climate models and estimation of the projected mean changes, this has limited value for non-scientific circles, including stakeholders like governments, the economy, city councils, private companies, and the general public (e.g., Lemos et al. 2012; Hackenbruch et al. 2017). Recently, several studies targeted the development and application of user-oriented climate indices towards potential applications as climate services. One important conclusion is that the users' needs are quite specific regarding different societal sectors and interests, and thus the co-development of individual, specifically tailored user-oriented variables is important to warrant their applicability in practical terms (e.g., Buontempo et al. 2018; Schipper et al. 2019). Such climate indices are co-designed with end-users to translate and aggregate the information contained in the climate model data to assure their applicability in practice. Experience has shown that continuous interaction with the end-users is essential for the development of new climate indices and prototype climate services (Buontempo et al. 2020). The applications include predictions on seasonal (Buontempo et al. 2020) and decadal (Moemken et al. 2021) time scales, as well as climate projections (e.g., Hackenbruch et al. 2016; Hundhausen et al. 2023).

The relevance of climate change is now generally recognised by government agencies and the private sector, particularly in Europe (Biesbroek et al. 2010; Lee et al. 2015). According to a survey of 1062 municipalities across Germany in 2023, about 12% of the municipalities have a climate adaptation plan in place, about 23% are currently developing one, and 31% address the issue through other policy strategies (Umweltbundesamt 2024). But even if the relevant information is available, adaptation to climate change remains a complex and challenging task, especially for public authorities due to economic, political, and structural hurdles (Corfee-Morlot et al. 2011; Measham et al. 2011; Lehmann et al. 2015; Fünfgeld et al. 2023). According to a survey for local administrations in Baden-Württemberg (Hackenbruch et al. 2017), the most frequently mentioned barriers are the topic novelty and lack of personnel resources, finances, and time, which are closely associated with information deficits (Lehmann et al. 2015). Moreover, concepts like climate variability, change and impacts are often difficult to translate for decision makers (Hackenbruch et al. 2017), or not affordable for individual smaller municipalities (Fünfgeld et al. 2023).

Other than more general user-relevant climate indices related to temperature and precipitation (extremes), user-oriented climate indices can quantify the specific impacts of climate change (Alexander et al. 2006; Zubler et al. 2014; Schipper et al. 2016; Hasel et al. 2023) and thus play a key role in reducing the challenges of adaptation to climate change at regional and local level, as they are explicitly based on the requirements of local decision makers and provided in a form that can facilitate the development of specific and adequate adaptation measures (Hackenbruch et al. 2017). They represent a combination of various meteorological parameters and specific thresholds to quantify climate change impacts in an application-oriented manner (Schipper et al. 2019). They can be tailored to individual fields of action, for example, the agricultural sector, or can be more all-encompassing. According to Hackenbruch et al. (2017), the most urgent demand for information for municipalities in Southern Germany lies in the adaptation to heat extremes, but water availability issues have played an increasing role in recent years (Schuldt et al. 2020).

In the current study, we use the first transient CPM ensemble for Southern and Central Germany (KIT-KLIWA; Hundhausen et al. (2023)) to quantify the projected changes for user-relevant climate indices. This unique CPM ensemble, driven by different global climate models (GCM), encompasses four transient ensemble members under historical (1971–2005) and the RCP8.5 scenario forcing (2006–2100), enabling a more detailed quantification of the climate change signal and associated uncertainties (Hundhausen et al. 2024, 2025). Additionally to temperature and precipitation related climate indices, we cover a range of user-oriented climate indices relevant to various stakeholder applications to address the information requirements of the different stakeholders. The expectation is that this very high-resolution tailored climate information for present-day and future climate conditions will help the development of effective adaptation strategies by allowing intercomparison between different geographical regions and learning from the adaptation strategies of other regions which may expect similar climate change signals. The current study has three main objectives:

- Quantification of the climate change signal for a wide range of climate indices considering different global warming levels (Section 4).

- Quantification of the climate change signal for the major landscape types and different altitudes (Section 5).
- Estimation of the uncertainties in the derived climate change signals (Section 6).

The paper is structured as follows: Section 2 describes the climate model ensemble and bias adjustment approaches, while Section 3 describes the climate indices and the application strategy. The following sections focus on the analysis of the climate change indices for Central and Southern Germany (Section 4), specific characteristics for the major landscape types (Section 5), and the quantification of associated uncertainties (Section 6). Section 7 discusses the applicability of the climate change indices. A summary and discussion conclude the paper in Section 8.

2 | Data and Methods

In order to quantify the changes in user-relevant climate indices, the transient four-member regional CPM ensemble is used as the main dataset. A description of the model data, the validation against observational datasets, the bias adjustment approach, and the selection of the global warming levels is provided below.

2.1 | Observational Data

We use the high-resolution gridded observation dataset HYRAS (Rauthe et al. 2013; Razafimaharo et al. 2020) from the German Weather Service (DWD) for comparison with model data and subsequent bias adjustment. The spatial resolution of the HYRAS observation datasets corresponds to about 5 km for near-surface temperature (daily minimum, mean, and maximum values) and to about 1 km for precipitation (daily sums). The data were interpolated conservatively to the 2.8 km high-resolution model grid. In addition, for the temperature values, a height correction was performed, underlaying a vertical gradient of 0.0065 K/m.

To determine the global warming level corresponding to present-day climatic conditions, we use HadCRUT5, the new version of the Met Office Hadley Centre/Climatic Research Unit global surface temperature data set (Morice et al. 2021). The dataset has a resolution of 5° and encompasses the period 1850 to near real time, providing monthly averaged near-surface temperature anomalies relative to the 1961–1990 period. The historical period 1991–2020 corresponds to a global warming level of 0.95 K (GWL0.95).

2.2 | A Transient Convection-Permitting Climate Simulation Ensemble

The KIT-KLIWA CPM simulations (Hundhausen et al. 2023) were carried out primarily within the scope of the KLIWA project[1] and completed within the RegIKlim-ISAP project.[2] Four Coupled Model Intercomparison Project—Phase 5 (CMIP5; Taylor et al. (2012)) GCMs (see Table 1) provided boundary forcing for downscaling. These four selected GCMs cover a large part of the range of climate sensitivities of the CMIP5 GCMs (cf. Table 1, Nijsse et al. (2020)). All four models are roughly within the plausible range for the transient climate response, with CNRM-CM5 and MPI-ESM-LR in the middle range and HadGEM2-ES and EC-Earth in the upper range in terms of Equilibrium Climate Sensitivity (ECS). The downscaling was performed with the regional Climate Model (RCM) COSMO-CLM (CCLM, version: COSMO5.0_CLM9; Rockel et al. (2008)) in a consistent downscaling chain. Three consecutive nesting steps were performed: first to 50 km (0.44°) over Europe, second to 7 km (0.0625°) over Germany and finally to 2.8 km (0.025°) over Central and Southern Germany (see Figure 1b). To represent convection in CCLM, the Tiedtke-parametrization was applied (Tiedtke 1989). For the final nest, a convection-permitting setup was used (cp. Baldauf et al. 2011), where the parametrization for deep convection was switched off. All four downscaling chains were performed for the historical experiment (period: 1971–2005) and the RCP8.5 scenario (period: 2006–2100). The CPM simulations were performed in a quasi-transient way: the simulations were originally performed in 30-year time slices preceded by a 3-year spin-up (1968–2000, 2018–2050, 2068–2100). These time slices were later extended (2001–2020, 2051–2070) to provide a quasi-transient ensemble for the entire period (see Hundhausen et al. (2023) for details). This ensemble, driven by multiple GCMs at this high horizontal resolution (2.8 km) and long time period (1971–2100), is unique for Germany. Only data from the CPM simulations (2.8 km) is analysed here. The final analysis domain covers Central and Southern Germany as well as the Alps in the south and parts of France in the west of the domain. The analysis focuses on the German part of the domain. The largest part of the domain

TABLE 1 | Forcing GCM, realisation, Equilibrium Climate Sensitivity (ECS in °C; cf. Nijsse et al. (2020)), time period in which the different GWLs are reached, and reference for the CMIP5 GCMs downscaled for the ensemble.

GCM	Realisation	ECS in °C	GWL0.95	GWL2	GWL3	References
CNRM-CM5	r1i1p1	3.28	1998–2027	2032–2061	2054–2083	Voldoire et al. (2013)
MPI-ESM-LR	r1i1p1	3.66	1981–2010	2019–2048	2045–2074	Giorgetta et al. (2013)
EC-EARTH	r12i1p1	4.18	1985–2014	2019–2048	2046–2075	Prodhomme et al. (2016)
HadGEM2-ES	r1i1p1	4.64	1995–2024	2021–2050	2041–2070	Collins et al. (2011)
HadCRUT5			1991–2020			Morice et al. (2021)

Note: According to the HadCRUT5 dataset, the historical period 1991–2020 corresponds to GWL0.95.

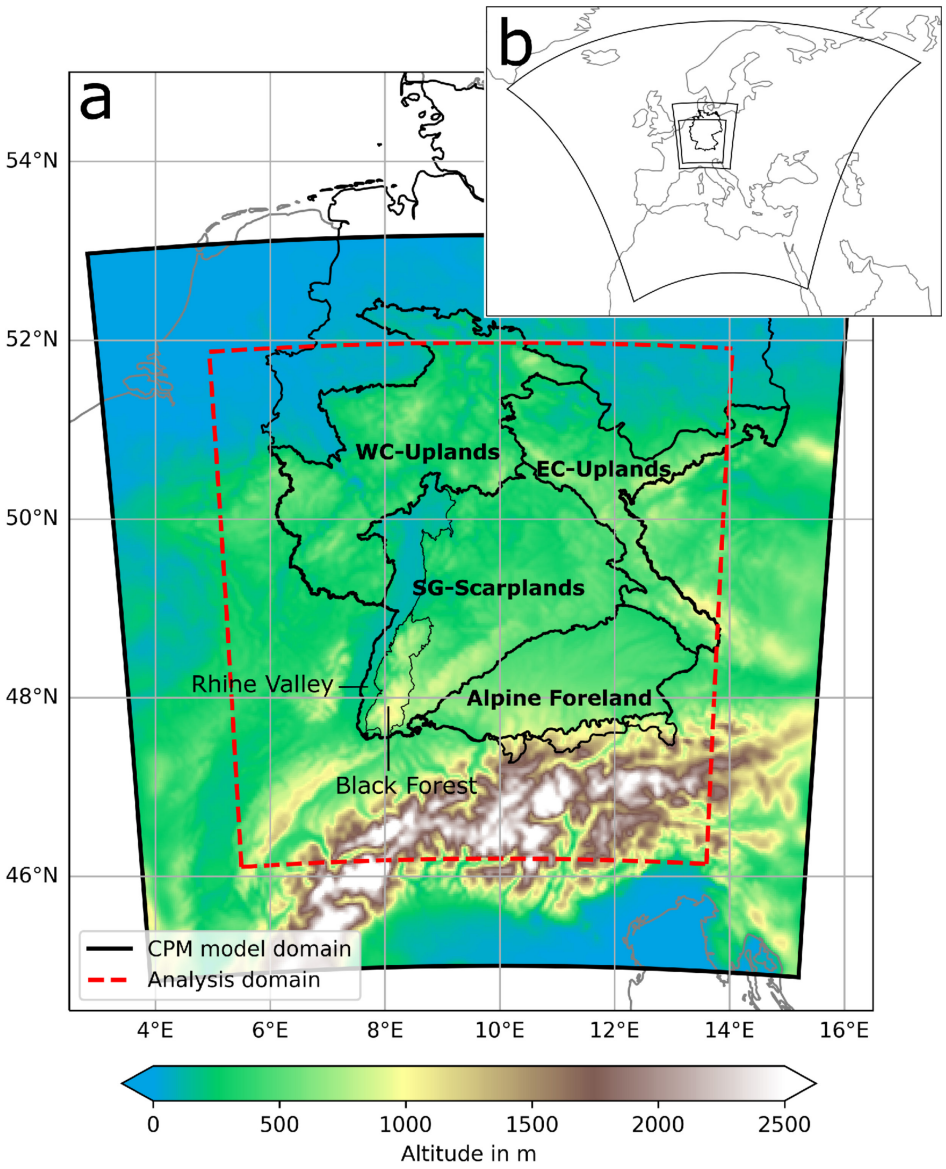

FIGURE 1 | (a) Analysis domain and the sub-regions considered (Alpine Foreland, South German (SG-) Scarplands, East-Central (EC-) Uplands, West-Central (WC-) Uplands, Rhine Valley, and the Black Forest). Altitude is indicated in colours. (b) shows the domains of the three nesting steps: 0.44° resolution outer domain, 0.0625° resolution intermediate domain, and 0.025° resolution CPM model domain. [Colour figure can be viewed at wileyonlinelibrary.com]

extends over the German region of low mountain ranges—the Western Uplands, the Eastern Uplands, and the South German Scarplands. The altitude of most of the low mountain ranges is between 500 and 1500 m. The Alpine Foreland covers the area in the south-east of Germany. It is a gently hilly area with altitudes of around 300–800 m.

2.3 | Bias Adjustment of the Model Data

A bias adjustment of the model data is essential for the current study, given that many indices are threshold-based and thus very sensitive even to small systematic biases. To remove the systematic biases of the distributions of the underlying variables for the index calculation, we apply the quantile delta mapping method described by Cannon et al. (2015) and coded by Schwertfeger et al. (2023) to the daily precipitation sums and the daily mean, minimum, and maximum temperature values. This bias adjustment is performed separately for each of the four ensemble members. The modelled distribution for the future 30-year time period is mapped to the observed distribution for the reference 30-year time period and scaled with the climate change signal given by the difference between the modelled historical and future distributions, assuming that a major part of the biases is stationary (e.g., Krinner and Flanner 2018). The change signal is added as absolute differences for temperature and multiplied as relative change for precipitation. The distributions are based on 100 quantiles for temperature and on 1000 quantiles for precipitation. In all cases, the HYRAS data (1991–2020, corresponding to GWL0.95) is used as a reference. Before bias adjustment, the uncorrected ensemble average 2-m annual temperature (Figure 2b) overestimates the HYRAS values (Figure 2a), while the mean average annual precipitation sum is overestimated by the uncorrected ensemble mean (cp. Figure 2d,e). Both

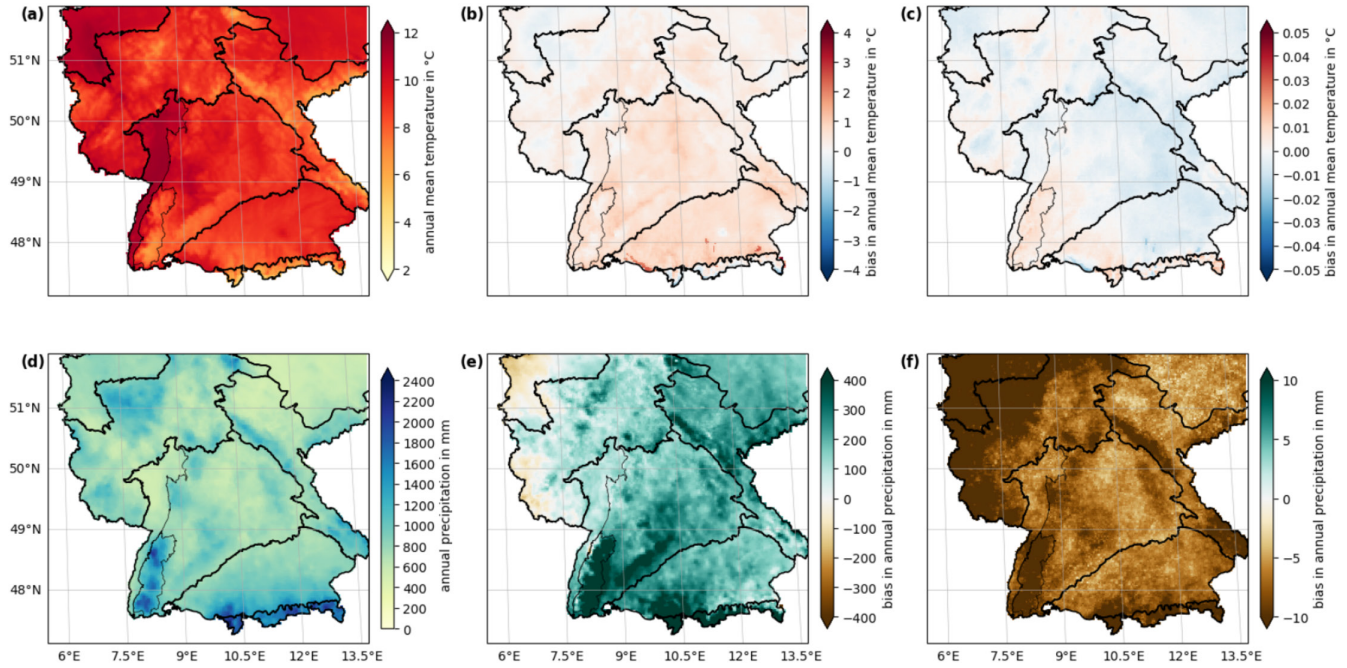

FIGURE 2 | Annual average 2 m temperature for (a) HYRAS 1991–2020 (GWL0.95), (b) bias in the ensemble mean of the uncorrected raw data for GWL0.95 compared to HYRAS, and (c) remaining bias of the corrected data. (d) Same as (a) but for average annual precipitation sums, (e) bias in the ensemble mean of the uncorrected raw data for GWL0.95 compared to HYRAS, and (f) remaining bias of the corrected data. Results for the single ensemble members are shown in Figures S1–S4. Note the different scale for the bias in the uncorrected and corrected data. [Colour figure can be viewed at wileyonlinelibrary.com]

biases are successfully removed by the bias adjustment method (Figure 2c,f). Nevertheless, small biases remain for precipitation (cf. Figure 2f). The analysis of the results for the single ensemble members (Figures S1–S4) reveals that this shortcoming is particularly associated with the HadGEM2-ES model (cf. Figure S3f).

2.4 | Global Warming Levels Definition

Following the recent IPCC (2023) report, we use the GWL concept to analyse our climate projections, as it facilitates the comparison between the different climate change signals and the quantification of regional and local impacts. A GWL is defined as the time range where the average global surface temperature increase relative to a pre-industrial time period exceeds a certain value. We use 1881–1910 as pre-industrial time period (see IPCC 2023), and we define a GWL+K as the first 30-year time period where the average global surface temperature increases by +K relative to this pre-industrial basis. The GWL time periods are determined specifically for each of the driving GCM and thus depend both on the GCM climate sensitivity and on the emission scenario. Using GWLs, at least part of the ensemble spread resulting from different climate model sensitivities is removed. In the present study, we focus on GWL2 and GWL3 (see Table 1). The choice of the RCP8.5 scenario was also justified by the choice of GWL3 as a target, for which a strong climate forcing is needed so that the selected 30-year period is within the simulated time period.

Slightly different definitions of GWLs have been described in recent peer-reviewed literature, typically focussing on a different definition of the pre-industrial time range, a change in the period's length or the reference period. For example, Vautard et al. (2014) and Teichmann et al. (2018) argued for the reference of 1971–2000, which corresponds to a GWL0.46 based on observational data. This approach was recently pursued, for example, in Hundhausen et al. (2023, 2024). In the present study, we have chosen 1991–2020 as a reference to enable a more straightforward applicability of the results for end users. According to the HadCRUT5 data (Morice et al. 2021), this period corresponds to a GWL of 0.95 K above pre-industrial conditions (1881–1910). Thus, we consider the historical time period for each GCM as GWL0.95 in the respective global driving simulation. These same observational reference and model historical time periods were also used in the bias adjustment process.

3 | User-Relevant Climate Indices and Strategy

This section describes the selection, calculation, and application of the different climate indices.

3.1 | Climate Indices Description

User-oriented climate indices can effectively quantify climate change (Alexander et al. 2006; Hasel et al. 2023) and help interpret its impacts on economy, ecology, and society (e.g., Zubler et al. 2014). Many indices have been proposed in the "Expert Team of Climate Change Detection Indices" (ETCCDI; Zhang et al. 2011), but many other region and sector specific developments followed (e.g., Alexander and Herold 2016; Hackenbruch et al. 2016; Schipper et al. 2016, 2019; Buontempo et al. 2018). User-oriented climate indices are applied across various sectors, such as transportation, public health, infrastructure, and

TABLE 2 | Definition of the climate indices, with TX: daily maximum temperature; TN: daily minimum temperature; TG: daily mean temperature; RR: daily precipitation sum.

Index	Input	Definition	References
Summer days (SU)	TX	Annual count of days with TX ≥ 25°C	[2–5]
Hot days (HD)	TX	Annual count of days with TX ≥ 30°C	[2,4,5]
Very hot days (VHD)	TX	Annual count of days with TX ≥ 35°C	[2,4,5]
Tropical nights (TR)	TN	Annual count of days with TN ≥ 20°C	[1–5]
Frost days (FD)	TN	Annual count of days with TN ≤ 0°C	[1–5]
Ice days (ID)	TX	Annual count of days with TX < 0°C	[2,3,5]
Heavy precipitation days (R10mm)	RR	Annual count of days with RR ≥ 10 mm	[1–3]
Very Heavy precipitation days (R25mm)	RR	Annual count of days with RR ≥ 25 mm	[2,4]
Extreme precipitation days (R40mm)	RR	Annual count of days with RR ≥ 40 mm	[2,4]
Snow days (SND)	TG, RR	Annual count of days with TG ≤ 1°C and RR ≥ 10 mm	[4]
Summer dry days (SDD)	RR	Annual count of days May–September with RR < 0.1 mm	[4]
Heating days (HD)	TG	Annual count of days with TG ≤ 15°C	[4,5]
Winter service days (WSD)	TN, RR	Annual count of days with TN ≤ 0°C and RR ≥ 5 mm	[4]
Hiking days (HID)	TX, RR	Annual count of days with TX < 25°C and RR < 5 mm, with TX > 0°C December–February, TX > 5°C March, November, TX > 10°C April, May, September, October, TX > 15°C June–August	[4]
Pollen washout days (PWD)	RR	Seasonal count of days April–September with RR ≥ 1 mm	[4]
Vegetation days (VD)	TG	Annual count of days with TG ≥ 5°C	[2,4,5]

Note: The thresholds used are often consistent across several references. However, some references differ in whether thresholds are defined using strict inequalities (greater/less than) or inclusive inequalities (greater/less than or equal to). In this case, we consistently use the inclusive form (≥ or ≤), in alignment with the definitions provided by the German Weather Service. Given the high precision of the simulation data, no significant deviations are expected between the two approaches. The definition of the indices is based on a sub-selection base on the following references [1] ETCCDI: Zhang et al. (2011); [2] Climpact: Alexander and Herold (2016); [3] European Climate Assessment & Dataset (ECA&D) Van Engelen et al. (2008); [4] KLIMOPASS: Schipper et al. (2016, 2019); [5] German Weather Service: www.dwd.de/DE/service/lexikon/Functions/glossar.html.

tourism, at different stages of the climate change adaptation process. In a first step, climate indices are commonly used to represent the current and future state of a system in terms of climate (Vogel et al. 2020). This provides insights into the systems conditions and raises awareness for potential risks. Second, they are applied to climate projections to quantify the changes (Frich et al. 2002; Alexander et al. 2006; Van Engelen et al. 2008; Hackenbruch et al. 2016; Schipper et al. 2019; Moemken et al. 2021; Hundhausen et al. 2023). In this study, we consider 16 user-relevant climate indices, including temperature indices (6), precipitation indices (5), and specifically developed user-oriented indices (5). A full list with details can be found in Table 2.

High and low temperatures can strongly impact human activity. Summer days (SU), hot days (HD) and very hot days (VHD) are defined as days with maximum temperature above or equal to 25°C, 30°C and 35°C, respectively. Analogously, tropical nights (TR) occur if the nightly air temperature remains above 20°C (see Table 2). The number of summer days, hot days, very hot days and tropical nights per year can be seen as different measures of heat stress on the human body. Excessive values can lead to increased health risks, especially for vulnerable groups, such as the elderly, children, or outdoor workers (e.g., Jendritzky et al. 2011). These four indices have been in use for decades, for example, at the German Weather Service,[3] to address specific stakeholder requests. Furthermore, we consider two indices associated with coldness to estimate impacts on energy consumption, construction and forest works, namely frost days and ice days. A frost day occurs if the minimum temperature lies below 0°C, while an ice day occurs if the maximum temperature lies below 0°C. The number of frost and ice days is very relevant for forestry and agriculture works. Frost can also damage roads, if water is able to seep into the surface through existing cracks.

Five different precipitation-associated indices are considered. The first three consider heavy (R10mm), very heavy (R25mm) and extreme daily precipitation (R40mm), with thresholds of ≥10, ≥25 and ≥40 mm/day, respectively (see Table 2). They are measures for intense precipitation which may lead to local flooding, backwater in sewer systems, and damaged infrastructure. The summer dry days (SDD) index accounts for days between May and September without precipitation (<0.1 mm/day), thus being an indicator for summer drought. Finally, snow days (SND) corresponds to days with average temperature below 1°C and >10 mm of precipitation, indicating thus substantial

snowfall that may hamper traffic and other activities, increasing the risk of roof collapses and forest tree damage.

Finally, five indices specifically developed for user-oriented applications are considered (see Table 2). In order to estimate the energy consumption of a building dependent of weather conditions, a heating day is defined as a day with mean daily temperature below 15°C, which is the heating threshold defined by the VDI Guideline 2067 (VDI 2012). A winter service day (WSD) is a frost day (daily minimum temperature ≤ 0°C) with at least 5 mm of precipitation (Schipper et al. 2016). The number of winter service days is of interest for the communities to plan the amount of salt needed for the streets and the personnel to drive the winter service cars, and in general for street safety. The number of hiking days (HID) is a measure for human recreation possibilities and comfort outside. We assume here that humans will probably go hiking if there is less than 5 mm precipitation and if the maximum temperature stays below 25°C (Schipper et al. 2019). A vegetation day is defined as a day with an average temperature above 5°C, representing the vegetation period. It is used to describe the growth of trees or agricultural crops and the development processes of temperature-sensitive ecosystems. Finally, pollen washout days quantify the number of days between April and September with significant precipitation (≥ 1 mm). The assumption is that precipitation can lead to lower pollen levels and thus alleviate the impacts on human health, for example, for persons with allergies (Schipper et al. 2016).

3.2 | Application Strategy, Validation and Statistical Tests

Following the bias adjustment of the climate model data and the selection of the different GWL periods, we now analyse how well the climate indices derived from the CPM simulations for GWL0.95 (representative for 1991–2020) agree with the same calculations based on the HYRAS dataset and thus facilitate their interpretation by stakeholders. For this evaluation and most of the posterior analysis, the four simulations are combined to a small ensemble. The ensemble mean is taken as the best estimate (Sections 4 and 5), and the deviations between the four simulations are used to quantify the uncertainty (Sections 5 and 6). Figure 3 shows exemplarily the average number of hot days (Figure 3a), heavy precipitation days (Figure 3c), winter service days (Figure 3e), and vegetation days (Figure 3g) per year as calculated from the HYRAS dataset. The corresponding difference between the ensemble mean and the HYRAS dataset are shown in Figure 3b,d,f,h, revealing only very small differences. However, some biases remain, particularly in areas of high altitude (e.g., R10mm and winter service days, Figure 3d,f). The comparison for the remaining indices is shown in the Figures S5–S7, where again most of the small remaining deviations are found over high altitude. A special case is pollen washout days and summer dry days, which both show a clear bias in the North-west area of the domain, reaching deviations of about 10% for the latter. This hints at shortcomings in the precipitation bias correction (cp. Figure 2f) and particularly for the dry day correction. In spite of these identified regional shortcomings for single variables, the estimated climate indices from the CPM ensemble are found to be sufficiently close to the values derived from HYRAS to enable the derivation of realistic climate change signals for end-users. This is particularly true if we consider area averages (see Section 4). We will thus use them in the following chapters. As we focus on bias-adjusted simulations, we do not assess the added value between datasets of different resolutions. Previous evaluations based on uncorrected simulations (Hundhausen et al. 2023, 2024) have already shown improvements from CPM, including a reduced cold bias in daily temperature—especially in summer—and a more realistic distribution of precipitation.

Additionally to the area maps based on the grid points (Figure 3), we calculate area means for geographical regions determined mainly by topography, the so-called major landscape types, such as BfN (2015); Ssymank (1994), to facilitate its use by end users. They enable policy makers to get a compact overview of the climate change signal in their region, or to compare the projected future development in their own region with others (within Germany). We consider the four major landscape types in the model domain, namely (1) Alpine Foreland, (2) South German Scarplands, (3) East-Central Uplands, and (4) West-Central Uplands. Moreover, two smaller neighbourhoods but very contrasting regions are considered, (5) the Rhine Valley and (6) the Black Forest (cf. Figure 1a).

We assess the significance of possible mean changes by applying the non-parametrical Mann–Whitney–Wilcoxon test (Wilcoxon 1945; Mann and Whitney 1947; D. Wilks 2020). The test is based on a shift of ranks, and we use samples of 120 (30 years × 4 members) for the test the significance at 5% and 1% levels when comparing the distributions from historical (GWL0.95) to future time slices (GWL2 or GWL3). For Figures 4 and S8–S10, a spatial correction of the significances is performed with the False Discovery Rate Method (Benjamini and Hochberg 1995; D. S. Wilks 2016). For regional aggregated assessments (Figures 5 and 7 and S15–S17), indices are regionally averaged before applying the test.

4 | Overview of Climate Change Signals

In this section, we provide an overview of the climate change signals for the different climate indices for the German part of the analysis domain (Figure 1). Both GWL2 and GWL3 are considered, and only changes in mean values are assessed. Possible changes in uncertainty are analysed separately in Sections 5 and 6. The contour plots of the climate indices and their projected changes provide a first overview of the regional differences in the German part of the model region, focussing on the four exemplary variables (Figure 4). They were chosen from the sample of 16 indices in order to cover both a wide range of applications and diverse climate change patterns (see following sections). The changes in the number of hot days show some spatial structure for GWL2, which considerably increases in magnitude and significance for the whole study area with GWL3 (Figure 4c). The largest absolute increases are clearly found in the lower, flat areas like the Rhine Valley, with up to +16 days/year. For heavy precipitation days (R10mm), small increases with similar magnitude are found for GWL2 and GWL3, but without a clear spatial structure or significance (Figure 4e,f). Regarding winter service days, a general reduction is found over mountainous regions, which is considerably stronger for GWL3, where

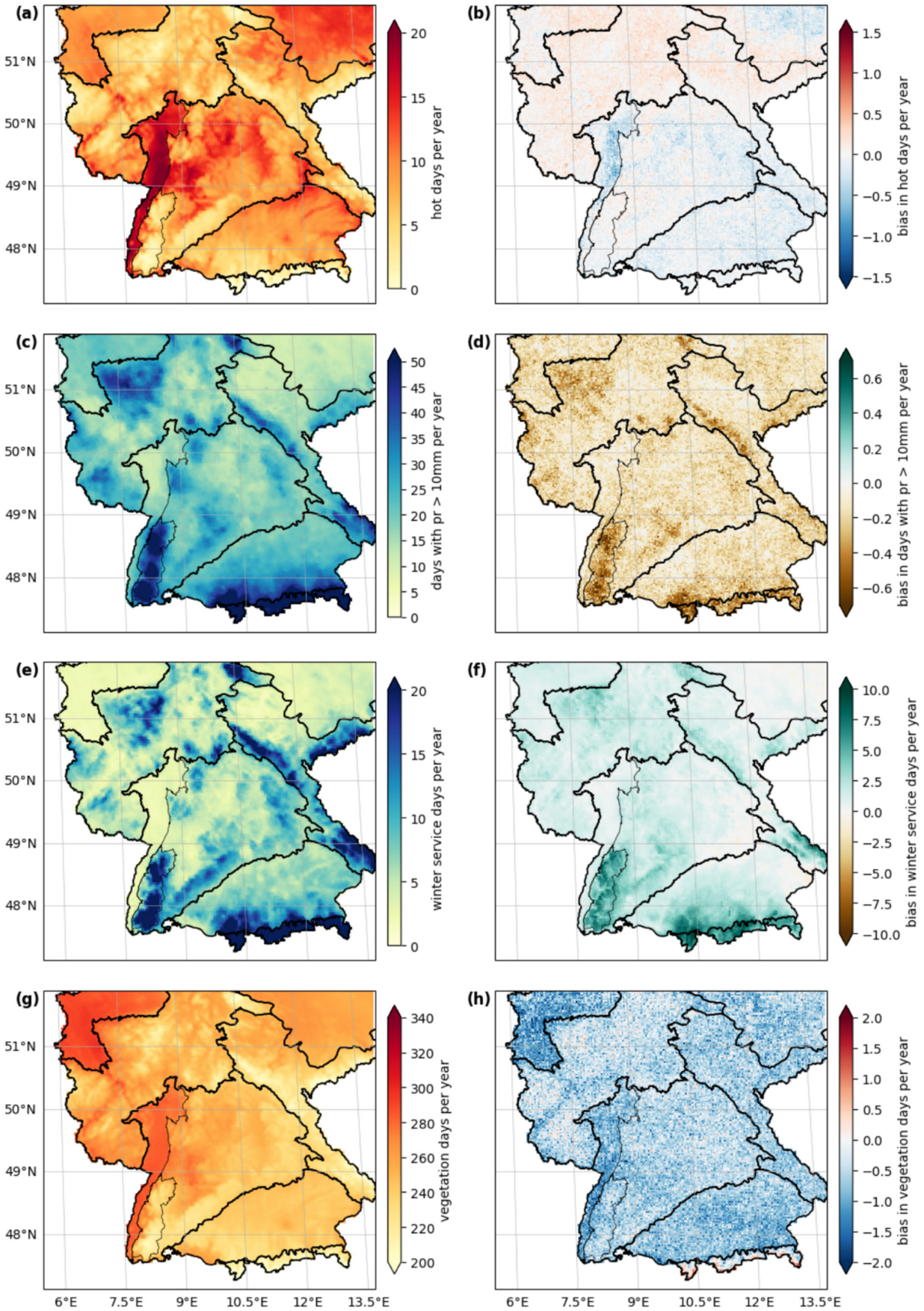

FIGURE 3 | (a) Average number of hot days for HYRAS (1991–2020, GWL0.95), (b) ensemble mean bias for hot days and GWL0.95 after bias adjustment, (c, d) same as (a, b) but for heavy precipitation (R10mm), (e, f) same as (a, b) but for winter service days, and (g, h) same as (a, b) but for vegetation days. The result of further climate indices is in Figures S5–S7. [Colour figure can be viewed at wileyonlinelibrary.com]

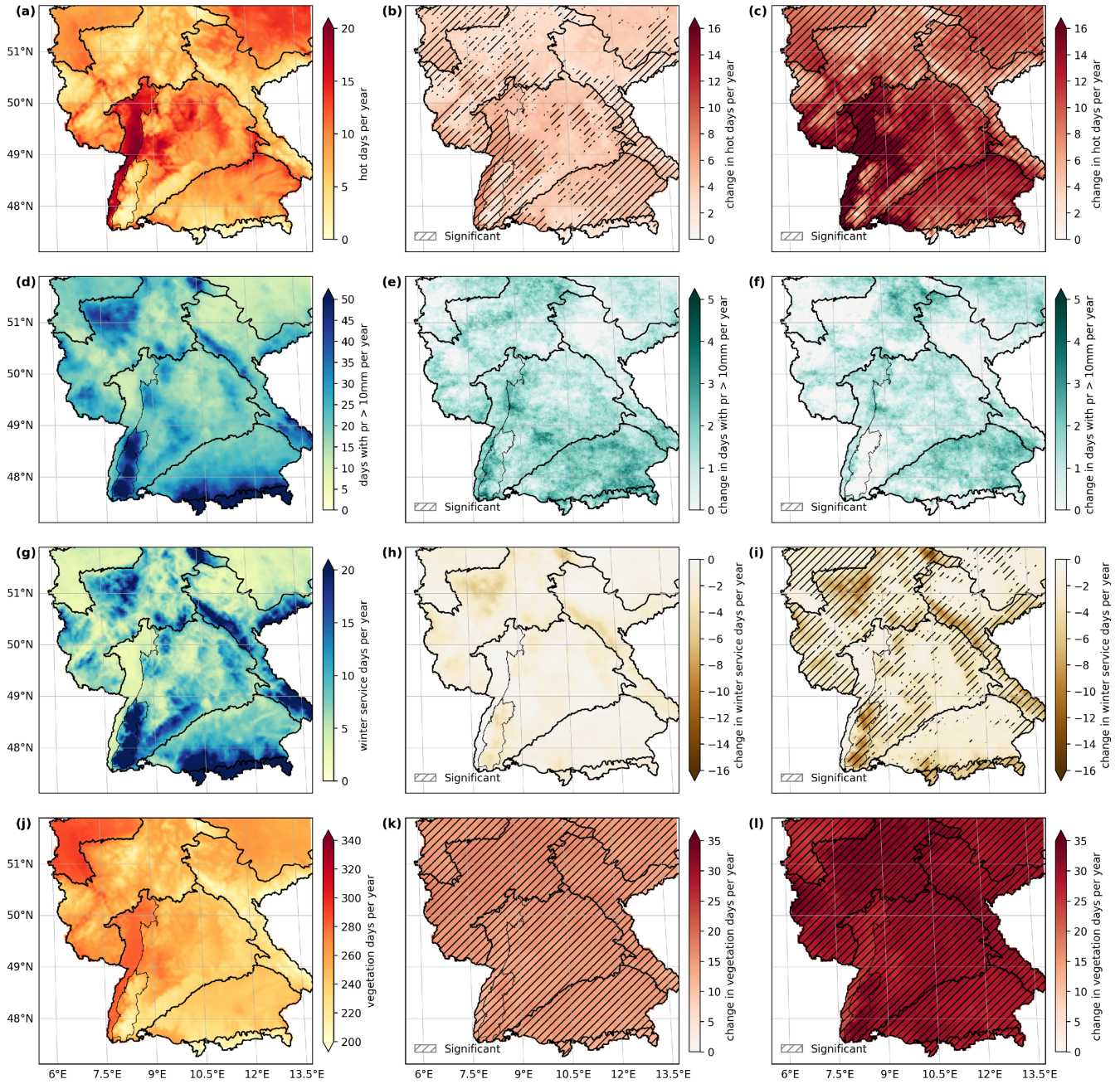

FIGURE 4 | (a) Ensemble mean of average number of hot days for GWL0.95, (b) difference between GWL2 and GWL0.95, (c) and difference between GWL3 and GWL0.95. Absolute differences were preferred for clarity. (d–f) same as (a–c) but for heavy precipitation (R10mm), (g–i) same as (a–c) but for winter service days, and (j–l) same as (a–c) but for vegetation days. The other indices are provided in Figures S8–S10. Significant changes at a 5% level of significance are indicated by hatching. [Colour figure can be viewed at wileyonlinelibrary.com]

significant changes are displayed for some areas (Figure 4i). Regarding vegetation days, a homogeneous increase is found with global warming, spatially fully significant for both GWL2 and GWL3, reaching about +35 days/year for GWL3 (Figure 4l).

The remaining variables are shown in Figures S8–S10. The indices based on temperature only, that is, the number of summer days, very hot days, and tropical nights, show generally an increase with increasing global warming and often statistically significant changes particularly for GWL3 (Figure S8). Although for summer days there is little spatial structure, regional differences are exacerbated for very hot days and tropical nights. This is particularly the case in the Rhine valley and also in other lower-altitude regions, where strong increases are already projected for GWL2, but even stronger for GWL3 (Figure S8). In some cases, relative changes exceeding +600% are reached (not shown). The number of frost days and ice days significantly decreases for GWL2, with stronger magnitude for GWL3, particularly in mountainous regions and the eastern part of the domain (Figures S8 and S9). Moreover, a non-significant reduced number of snow days occurs over high orography regions for GWL3 (Figure S9). The number of hiking days generally increases, with a clear focus on elevated areas, with larger changes in the northern

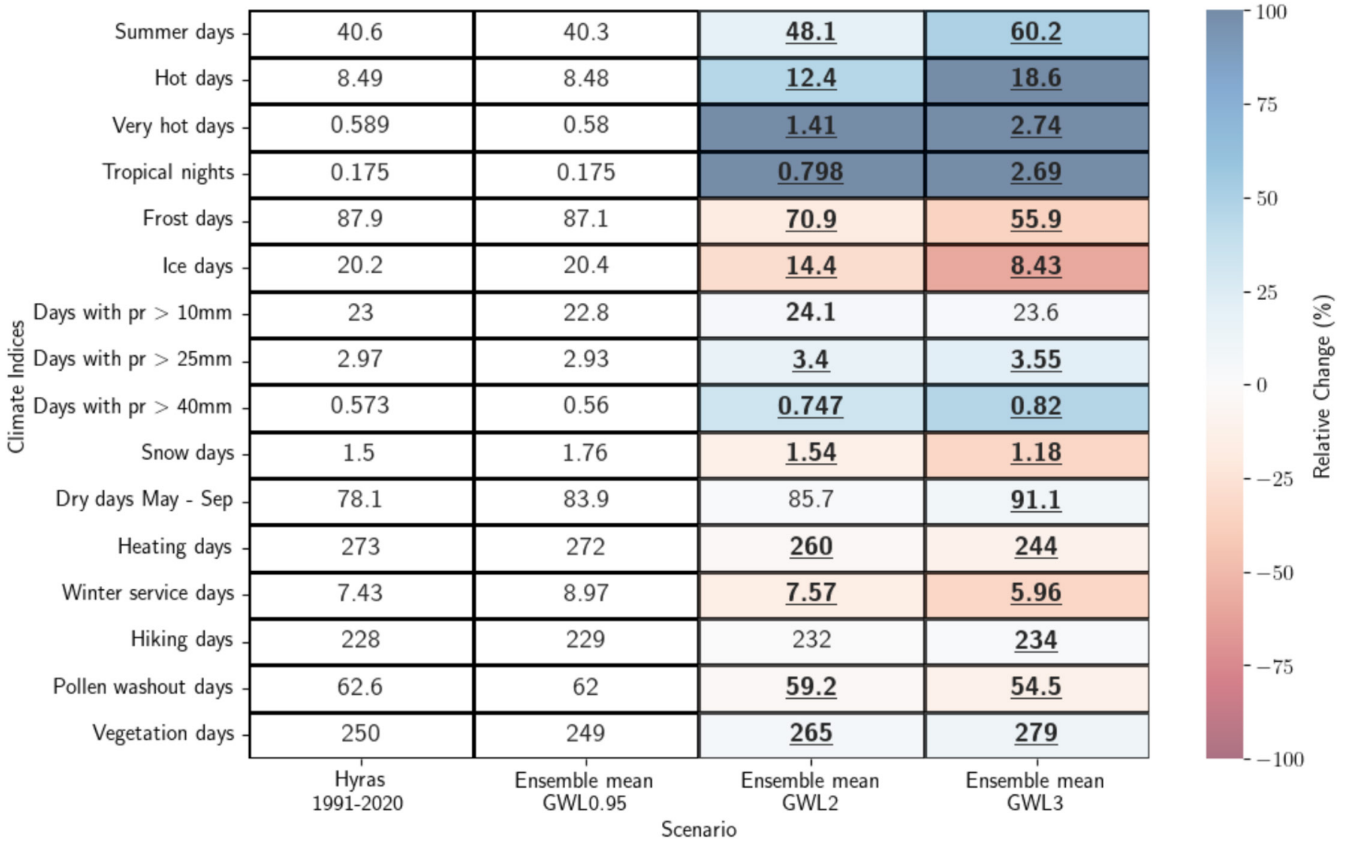

FIGURE 5 | Spatial average of the 16 climate indices over the analysis domain for HYRAS 1991–2020 (GWL0.95), ensemble mean for GWL0.95, GWL2, and GWL3, respectively. Statistically significant differences between GWL2 and GWL3 to GWL0.95 at the 5% significance level are indicated in bold; those reaching the 1% significance level are also underscored. [Colour figure can be viewed at wileyonlinelibrary.com]

and eastern parts of the domain (Figure S10). The number of summer dry days slightly increases and the number of pollen washout days decreases, particularly on the western part of the domain and GWL3 (Figure S10). Here, interpretation should be careful given the shortcomings with the bias adjustment (see Section 3). Even if the number of heavy precipitation days shows little spatial structure in terms of climate change (Figure 4e,f), very heavy and extreme daily precipitation does show spatial structure, projecting a non-significant increase in the Black Forest and Alpine regions (Figure S9), providing an indication of enhanced extreme precipitation events in the future. Conversely, the average heating days values significantly decreases with increasing global warming, but show little spatial structure (Figure S10).

The results are summarised for the whole area in Figure 5, which includes the spatial average values for all 16 indices for the whole study area for present day (GWL0.95), GWL2 and GWL3. As a reference, the HYRAS based results are also included in the first column. The present day values compare extremely well with HYRAS in terms of area averages, with the exception of summer dry days (+7%), snow days (+17%) and winter service days (+20%), which are related to the remaining biases in precipitation discussed in Section 3. In terms of the impact of global warming, several different patterns can be observed: for hot temperature related indices, a general and significant increase is found. The higher the threshold, the higher the relative changes because of rather small numbers for the current climate, with very hot days reaching over +100% already for GWL2. Even more prominent are the relative changes for tropical nights, which—starting from a very low value for present day—increases ×15 for GWL3. On the other hand, the average number of frost days and particularly of ice days is reduced, with a significant reduction exceeding 50% for GWL3 for the latter. For precipitation indices, both an increase of area averaged summer dry days and days with heavy, very heavy, and extreme precipitation are found. The relative changes are highest and significant for the more extreme indices, suggesting a shift to more convective precipitation in the region in a warmer climate (Da Silva and Haerter 2025). The number of summer dry days shows a small increase, significant for GWL3. On the other hand, and as expected, the number of snow days and winter service days decreases considerably, both showing a reduction of −30% for the study area. A small but significant decrease is found for heating days and pollen washout days, which show slightly decreased numbers with increasing global warming. The area averaged number of hiking days slightly but significantly increases for GWL3 (see Figure S10). Finally, a significant increase is found for vegetation days, with relative changes exceeding 12% for GWL3 (Figure 5).

5 | Regional Evaluation for Major Landscapes Types

In this section, we provide an overview of the climate change signals for the different climate indices for the whole study

area and the six defined regions, including the four large major landscape types—namely (1) Alpine Foreland, (2) South German Scarplands, (3) East-Central Uplands, (4) West-Central Uplands—plus Rhine Valley and Black Forest (see Figure 1). Special attention is given to the sometimes subtle differences between the four ensemble simulations. In order to provide a succinct overview, the main focus is given to four exemplary indices: hot days, heavy precipitation days, winter service days, and vegetation days (analogue Figures 3 and 4) for both GWL2 and GWL3.

The results for the average annual number of hot days and the six regions plus the whole model area are depicted in Figure 6a. The Box–Whisker plots present the median and inter-quartile-range of values for the correspondent 30 year periods (GWL0.95, GWL2, GWL3). The range of the four simulations is indicated for each region, following the order and shading indicated on the insert of the far right side. Analysing first GWL0.95 for the whole model region (in grey), we observe that the median and range are slightly different between the four ensemble members. This observation generally applies for the six regions, where HadGEM-2 often shows a large inter-quartile range, and MPI-ESM a somewhat skewed distribution. For GWL2 (in yellow) and GWL3 (in red), a general, systematic increase is found in all regions, in line with the changes for daily mean and daily maximum temperature in the simulations (Figure S11a,b). Small differences are found between GCMs, with HadGEM2-ES typically showing higher relative changes, particularly for GWL2. The largest relative changes are found for the Black Forest and GWL3 (Figure S11a–c).

For heavy precipitation days (Figure 6b), mean values are around 15–30 days per year in all cases for GWL0.95, except for the Black Forest, where about 45 days a year on average are recorded for the four models. In all cases, small changes in the number of heavy precipitation days are found, generally indicating a small increase but lacking clear consistency both in terms of the differences between regions or GWLs (in line with Figure 4e,f) and the general changes in precipitation in the simulations (Figure S11d). The changes in winter service days depend both on temperature and precipitation, and thus provide a more complex pattern (Figure 6c). The spread between the four simulations is comparatively large for GWL0.95 (Figure 6c), but in all cases a systematic decrease for GWL2 and GWL3 is found, particularly for model CNRM-CM5, which again shows the largest decrease by comparatively small inter-quartile-range (e.g., Rhine Valley). For vegetation days, notable differences are also seen between the ensemble members for GWL0.95. In all cases, there is a systematic increase for GWL2 and GWL3, with CNRM-CM5 displaying the larger absolute changes, and often smaller inter-quartile range (e.g., Rhine Valley).

The other variables are shown in Figures S12–S14. For tropical nights, a very large increase is identified for the Rhine Valley and GWL3. For the other regions, enhanced numbers are also found, but starting from very low values for GWL0.95. This result agrees well with the changes in daily minimum temperature (Figure S11c). Regarding frost days and GWL0.95 (Figure S12), the four models show small differences, and in particular very large inter-quartile-ranges for the Rhine Valley. Here, considerable differences are identified between the models for GWL2 and GWL3. The model CNRM-CM5 shows for all regions the strongest reduction on frost days, showing in some cases a reduction by 50%, and a smaller inter-quartile-range. For the other models, changes are weaker, particularly for MPI-ESM, with typically a large inter-quartile-range. For very heavy and extreme precipitation days (Figure S13), the relative changes are more prominent than for heavy precipitation days, now with values reaching around +25% for GWL3, and with stronger enhancements for CNRM-CM5 (e.g., West-Central-Uplands). A final example is hiking days (Figure S14), which shows quite interesting patterns of change. While wide inter-quartile-ranges are typical for all regions and GWLs, small upward trends are identified for the East-Central Uplands and the West-Central Uplands, particularly for GWL3 and CNRM-CM5. On the other hand, in regions like the Rhine Valley, there is a considerable decrease for GWL3, even if the changes for GWL2 are not clear. These results are in line with results from Section 4.

We now look in more detail at the changes for four exemplary variables and the six regions (Figure 7). Included are the area average values for hot days (Figure 7a), heavy precipitation days (R10mm, Figure 7b), winter service days (Figure 7c) and vegetation days (Figure 7d) for present day (GWL0.95), GWL2 and GWL3. As a reference, the HYRAS-based results are also included in the first column. Regarding hot days (Figure 7a), the changes for GWL2 are moderate (about 20%–30%) but already statistically significant in all cases, with the smallest relative changes for the Rhein Valley and the largest for the Black Forest. This pattern is intensified for GWL3, where the changes for the Black Forest reach +70% and for the Rhine Valley about +40%, and the four major landscape types between these values. When considering heavy precipitation days (Figure 7b), increases are found for all six regions, but they are relatively small. The Rhine Valley features the smallest absolute change but also the largest relative change. Given the small numbers, a careful interpretation is needed. Still, the results are a clear indication that an increase of very heavy precipitation in a warmer climate is found for all six regions. Unlike the two above variables, notable differences between GWL0.95 and the HYRAS reference data are found for winter service days (Figure 7c). This is particularly the case for the Black Forest. Regarding the climate change signal, a general and significant reduction is found both for GWL2 and GWL3, with the latter indicating reductions of about −40% or more. However, given the small numbers in some regions (particularly for the Rhine Valley), and the identified bias compared to HYRAS, the magnitude of the changes should be regarded with care. Finally, a consistent, relatively homogeneous and statistically significant increase is found for vegetation days, ranging between 10% to 13% for all six regions and GWL3.

Regarding other variables (Figures S15–S17), the largest changes are found for tropical nights, which—starting from very low values everywhere—often increase by 10× values for GWL3, but to a lesser extent in the Rhine Valley and West-Central Uplands for GWL2 (Figure S15). On the other hand, frost days (Figure S15) display a consistent and systematic decrease with numbers is found with enhanced global warming. This is true for all six regions and both GWLs. The reduction in the number of frost days is particularly prominent for the Rhine Valley and West-Central-Uplands, with values of about −40% or more for GWL3. The same is true for ice days, with a reduction

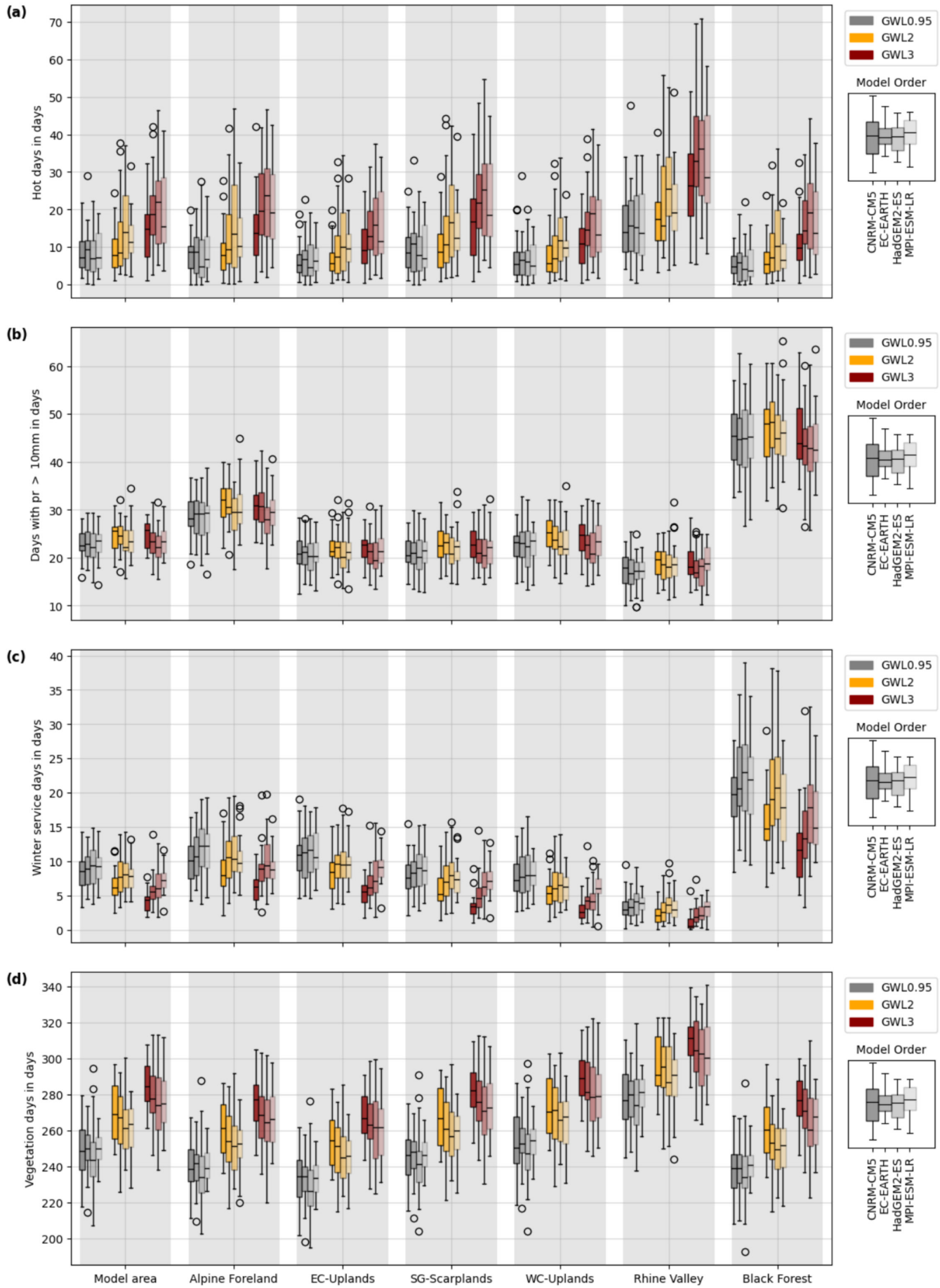

FIGURE 6 | Legend on next page.

FIGURE 6 | Box–Whisker-plots for (a) average number of hot days for the whole study area, Alpine Foreland, South German Scarplands, East-Central Uplands, West-Central Uplands, Rhine Valley and the Black Forest. For each region, the range of the four ensemble model simulations is indicated, following the order and shading indicated on the insert of the far right side. GWL0.95 is shown in grey, GWL2 in yellow, and GWL3 in red. (b) as (a) but for heavy precipitation days; (c) as (a) but for winter service days; (d) as (a) but for vegetation days. The results for the basic variables and other indices are provided in Figures S11–S14. [Colour figure can be viewed at wileyonlinelibrary.com]

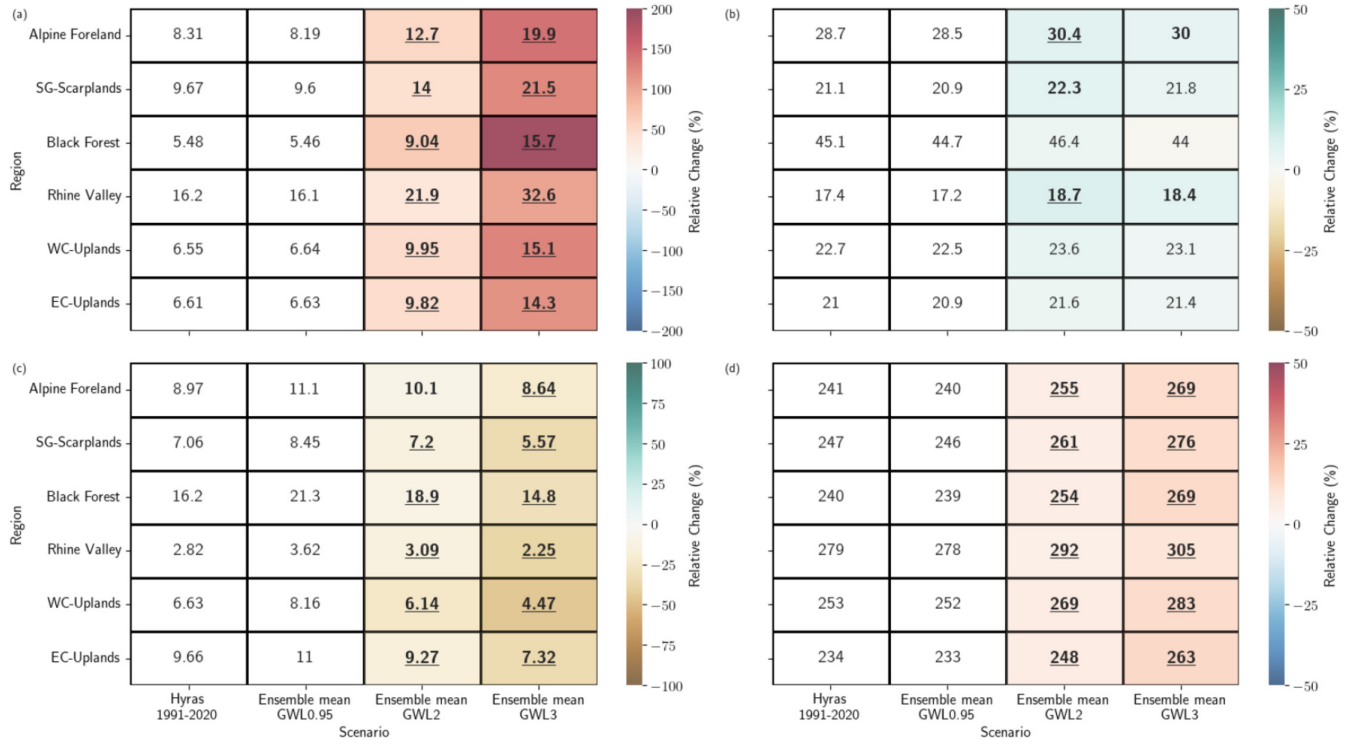

FIGURE 7 | Spatial average of the climate indices in HYRAS and the ensemble mean for GWL0.95, GWL2, and GWL3 in the different focus regions. The climate indices (a) hot days, (b) heavy precipitation days (R10mm), (c) winter service days, and (d) vegetation days are shown. The results for the other indices are provided in Figures S15–S17. Statistically significant differences between GWL2 and GWL3 to GWL0.95 at the 5% significance level are indicated in bold; those reaching the 1% significance level are also underscored. [Colour figure can be viewed at wileyonlinelibrary.com]

of about −75% for the Rhine Valley and GWL3 (Figure S16). Finally, the number of days with very heavy precipitation (R25mm) and extreme precipitation (R40mm) increases with global warming in all regions, and particularly for the Rhine Valley, where R40mm roughly duplicates both for GWL2 and GWL3. In contrast to R10mm (Figure 7b), changes in R25mm and R40mm are significant throughout all regions analysed with a level of significance of 5%, and almost always for a level of significance of 1%.

6 | Uncertainties in the Climate Change Signals

Given that we have a 4-member model ensemble and 30-year periods for each GWL, we now analyse in detail the model-related uncertainty and the resulting spread for the climate indices. We first take a closer look at the four core basic variables for the computation of the indices. Figure 8 shows the variability of the time series for the three different 30-year periods, namely GWL0.95 (grey), GWL2 (yellow), and GWL3 (red). The model range is indicated by shading in the corresponding colour, and the highest value for each model is indicated with a specific icon (see legend). The mean and median values for each variable and GWL are indicated in Table S1.

For the three temperature variables (Figure 8a–c), the climate trend over the 30-years periods is apparent as the mean values—dashed horizontal line—clearly change between the GWLs (cf. Table S1). Moreover, the most extreme values are—with one exception for CNRM-CM5 and GWL2—all found in the mid-decade or the last decade of the period, indicating a trend within the 30-year period. This is particularly the case for GWL3, where all the largest values per model fall within the last 8 years. Regarding daily maximum temperature (Figure 8b) and daily minimum temperature (Figure 8c), they closely follow the pattern identified for the daily mean temperature (Figure 8a). Of notice are the large changes in terms of mean values for the 30-year periods (horizontal dashed lines), of roughly one K per GWL. The maximum for CNRM-CM5 and GWL2 remains the only extreme value in the first 10 years. Interestingly, there is no indication that the diurnal temperature range changes with global warming. The differences between maximum and minimum temperatures lie between 8.71°C and 8.82°C for all GWLs and both mean and median values (cf. Table S1). Figure 8d shows the same information but for

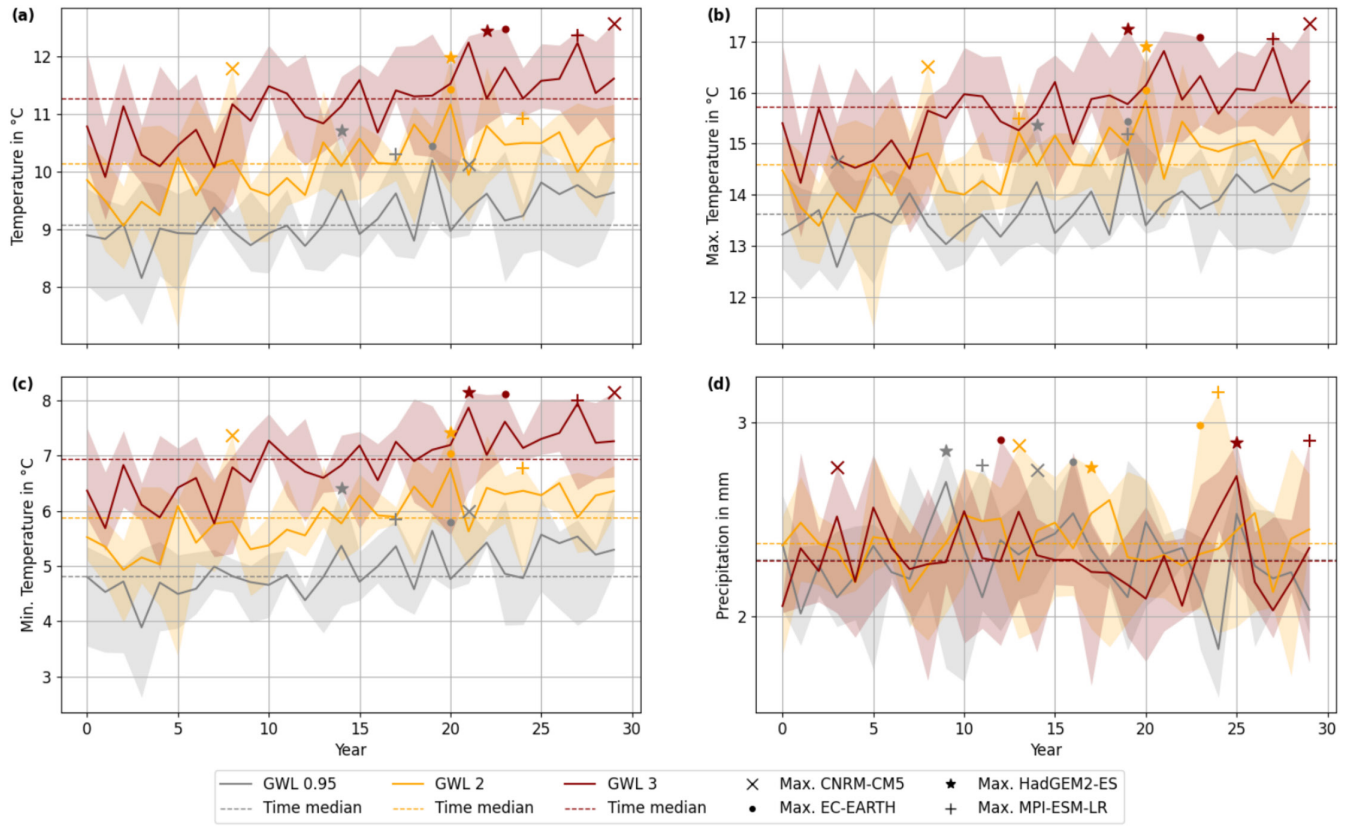

FIGURE 8 | Time series of annual average (a) daily mean temperature for GWL0.95 (grey), GWL2 (yellow), and GWL3 (red). Indicated are the median of the four simulations (line), the range between the simulations (shade) and maximum and minimum values for each model (symbols). The median and mean values for GWL are indicated in Table S1. (b) as (a) but for daily maximum temperature; (c) as (a) but daily minimum temperature; (d) as (a) but for daily precipitation. [Colour figure can be viewed at wileyonlinelibrary.com]

precipitation. Here results are more mixed: while the mean value for GWL2 is slightly higher, the values for GWL3 and GWL0.95 are almost identical. Instead, a large year-to-year variability dominates, with the largest single model values often found in central decade, followed by the last decade. Only two largest values are found in the first 10 years, namely for CNRM-CM5 and GWL2, and HadGEM2 for GWL0.95. Notable is also the particularly large spread for GWL2 in the last decade.

Regarding now the four selected indices (Figure 9), hot days (Figure 9a) show an increasing trend in terms of mean values. With two exceptions only, the maximum values for each simulation are found in the second half of the time series. The variability between the four simulations is also particularly large for GWL3 (red), primarily in the second half of the time series. For heavy precipitation days, the pattern of change is not so clear. While the mean value for GWL3 is slightly higher than GWL0.95 and GWL2, the variability is very large and no apparent trends can be observed within the 30-year blocks. This is in line with the results shown in Figure 4e,f. On the other hand, considerable changes are identified for winter service days: there is a clear decrease in the mean values with increasing global warming, and the maximum values for the individual simulations are typically found in the first half of the time series, thus suggesting downward trends. Vegetation days show the opposite behaviour, with increasing mean values with GWL and an enhanced frequency of maximum values in the last decade. This is in line with Figures 4 and 5.

Regarding other variables (Figures S18–S20), the magnitude of change is particularly large for very hot days and tropical nights. Very prominent is the increasing spread for GWL3, particularly for tropical nights (Figure S18). For summer dry days and hiking days, moderate increases are found (Figure S20). The pattern for very heavy precipitation and extreme precipitation shows an increase in mean values and increased variability. For frost and ice days (Figure S19), a clear decreasing trend is found for the time series, together with a large spread between the models. Of note is the fact that the maximum single model values are practically all found in the first half of the time series for GWL2 and GWL3 (unlike GWL0.95). On the other hand, the number of Pollen washout days shows a small decrease with warming, with almost all extreme values being found in the first half of the time series (Figure S20).

7 | Applicability of Climate Change Indices

In the following, we discuss the relevance and applicability of the above results for different stakeholders. The study area will be experiencing a strong increase in hot days and very hot days, and unprecedented changes for tropical nights. The Rhine Valley is already experiencing the highest number of hot days and tropical nights among all the regions analysed, and thus local authorities are already under increasing pressure to adapt to the negative effects of heat. Excessive heat stresses the human body and endangers people with pre-existing

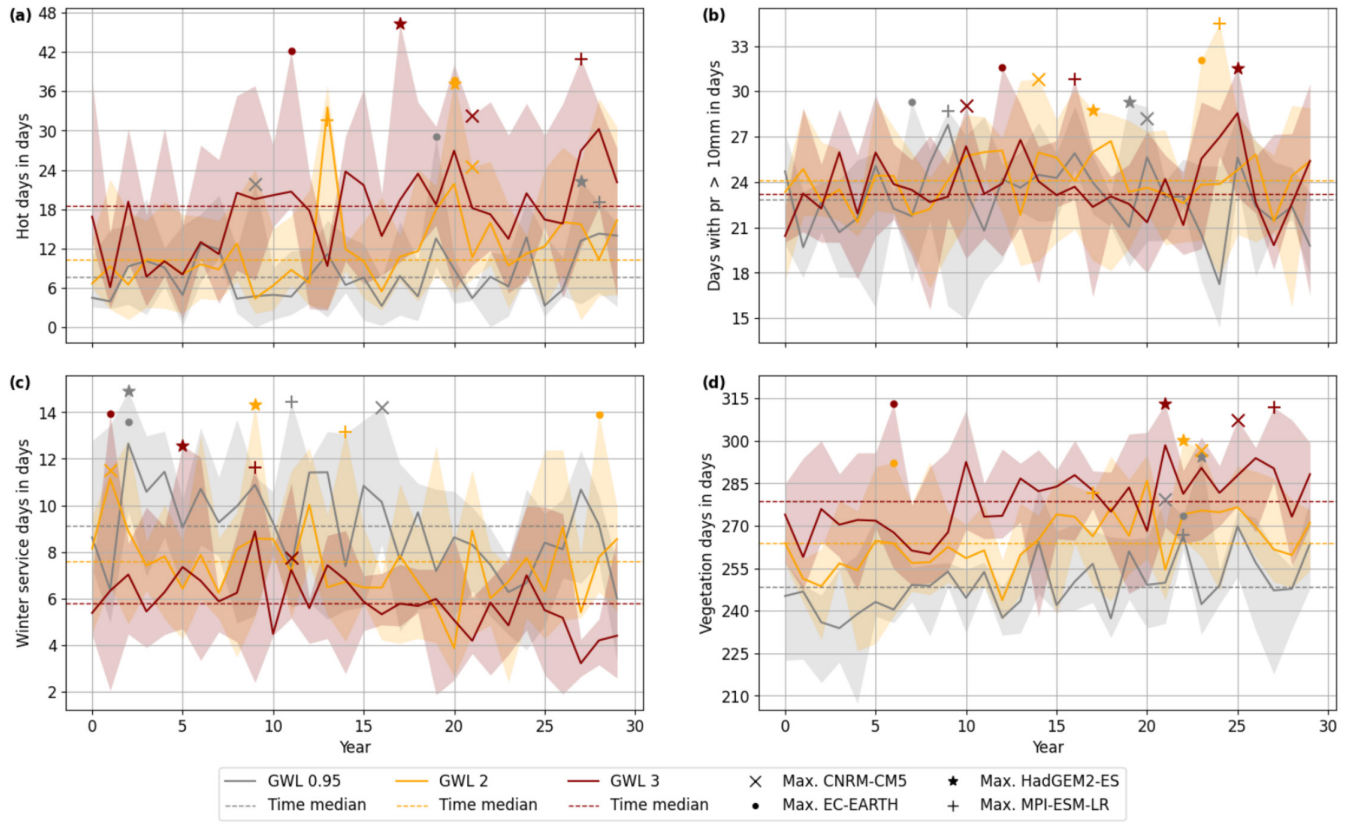

FIGURE 9 | Time series of (a) the average annual number of hot days for GWL0.95 (grey), GWL2 (yellow), and GWL3 (red). Indicated are the median of the four simulations (line), the range between the simulations (shade) and maximum and minimum values for each model (symbols). (b) as (a) but for heavy precipitation days; (c) as (a) but winter service days; (d) as (a) but for vegetation days. The results for the other indices are provided in Figures S18–S20. [Colour figure can be viewed at wileyonlinelibrary.com]

conditions, infants, young children, outdoor workers, and in particular elderly people. An overload of the body's own cooling system can lead to decreasing concentration, dehydration, and respiratory diseases to heat stroke, cardiovascular problems, and death (Kunz-Plapp et al. 2016; Schipper et al. 2019). Increasing hot days and tropical nights are therefore strongly related to increased premature mortality (Mora et al. 2017). Due to demographic change in Germany, with an increasing number of elderly people, heat stress will become an even more key topic (Cole et al. 2023). The local government of Karlsruhe (Rhine Valley) has developed a heat action plan that outlines specific adaptation measures, which have largely been implemented. For example, drinking water dispensers were installed at schools and in public buildings, such as hospitals. Due to increased heat and pollen occurrence, a higher risk to human health can thus be assumed in these regions. In higher regions currently not affected by heat extremes, a comparison with the current procedures for other areas using climate indices can simplify the risk assessment. For example, the Black Forest is not yet experiencing heat stress nor high pollen exposure. However, our results indicate a 70% increase in the number of hot days due to climate change. This would bring the number of hot days to the same level as currently found in the Rhine Valley. Local authorities in the Black Forest could thus profit from the available expertise and use the available information for the Rhine Valley as a guideline and adopt similar heat adaptation measures.

Our results also highlight extreme precipitation as an emerging challenge. The region will experience a significant increase in R25mm and R40mm on average (Figure 5), but little change was found for R10mm. In addition, the projected changes are not spatially homogeneous. The relative changes in extreme precipitation events will be particularly strong in high-altitude regions (Black Forest, Alps). In fact, both the frequency and the intensity of extreme precipitation are expected to rapidly increase globally and regionally with global warming (Winsemius et al. 2016; Alfieri et al. 2017; Papalexiou and Montanari 2019), with rates that can reach 7%–9% per degree of warming (Ludwig et al. 2023). As a result, even regions with a comparatively small number of heavy precipitation days (Rhine Valley) will need to implement adaptation measures, as such areas are often less prepared in terms of infrastructure, making targeted adaptation measures especially critical (Huang et al. 2021).

Climate indices also play a role in supporting decision-making and strategic planning in adaptation efforts, particularly if they were co-developed with stakeholders (Schipper et al. 2019; Vogel et al. 2020) and are thus closely aligned with adaptation needs. Our current results indicate that mountainous regions like the Black Forest and the Alps will experience the strongest decrease in winter service days, frost days, and ice days. In contrast, low-lying regions currently experiencing few cold days are expected to experience only minor changes. In regions with few winter

service days, even small shifts may require adaptations in winter service planning, for example, regarding the economic viability of investing in new vehicles. In contrast, the Black Forest or the Alps may have a higher threshold for triggering adaptation measures, as snow and ice clearance is needed throughout the winter season. Schipper et al. (2019) concluded that a 10% decrease in winter service days would trigger changes in terms of personnel planning, purchasing of deicing salt and new vehicles (Venäläinen and Kangas 2003). While this threshold cannot be directly applied to other regions, it can serve as a starting point for local decision-makers to determine the thresholds specific to their regions. By learning from regions with current exposure to conditions expected elsewhere in the future, targeted and experience-based adaptation measures can be more effectively developed and implemented.

8 | Summary and Conclusions

The current study aimed to demonstrate the usability of a CPM ensemble to quantify the climate change signal for a wide range of user-relevant climate indices for Central and Southern Germany. This was performed for different GWLs and landscape types, under consideration of model uncertainties. The main conclusions are as follows:

- The climate change signals were computed for many climate indices and different GWLs. For high temperature indices, a significant increase with global warming is found, particularly for very hot days and tropical nights, with an over 15-fold increase for the latter under GWL3. Conversely, the number of frost and ice days significantly decreases, again particularly for GWL3. Other indices like hiking days and summer dry days show only comparatively small though still significant changes in terms of area averages for GWL3.
- A more detailed view of the regional changes was achieved by the consideration of the major landscape types. Our analysis reveals that the relative changes will be considerably larger for elevated areas like the Black Forest for the various high temperature indices. Again, the number of tropical nights and very hot days increases by about 10-fold or more for this region under GWL3. However, the larger absolute changes are found in the Rhine Valley. Conversely, the Rhine Valley displays the larger relative changes in terms of very heavy and extreme precipitation, while the larger absolute changes are found in high elevation areas like the Black Forest and Alpine Foreland.
- The uncertainties of the climate change signal were estimated. For high-temperature indices, increasing trends for mean values and variability are found, with 30-year extremes typically found in the second half of the time-slices. The opposite behaviour is found, for example, for ice days, snow days, and winter service days. The increase in precipitation indices was found to depend crucially on the threshold considered, with stronger signals and greater variability in change occurring for higher precipitation thresholds. Finally, vegetation days show a rather steady increase in the number of days with global warming, but no apparent change in variability.

Among future pathways of research, it will be very interesting to explore this pool of results in detail for different seasons, in particular regarding the role of changing seasonality. Another pathway will be to investigate how far the identified changes in the user-oriented climate indices in the individual models can be related to possible changes in regional atmospheric circulation, for example changes in the North Atlantic Oscillation (Wanner et al. 2001), East Atlantic Pattern (Wallace and Gutzler 1981) and Weather Regimes (Vautard 1990).

The research included in this study is embedded in the RegiKlim project, which aims at generation, evaluation and provision of regional and local usable climate information for Germany, including the co-development of adaptation measures and impact quantification. One of the main insights of this project is that much more effort should be put into the co-design of user-oriented and locally adapted climate indices and knowledge transfer to local communities to achieve a truly climate-resilient society.

We conclude that this CPM ensemble can be an extremely useful tool for providing high-quality climate-related information to stakeholders, both for the recent past and future climate. The high spatial resolution allows an appropriate quantification of uncertainty ranges. Considering the applicability of the results, we conclude that the climate indices can effectively support decision-making and strategic planning for adaptation efforts on the regional and local scales, across various sectors and at different stages of the adaptation process. Therefore, climate indices can strongly contribute towards effective and timely planning and the implementation of adaptation measures.

Author Contributions

Joaquim G. Pinto: conceptualization; writing – original draft; writing – review and editing; methodology; funding acquisition. **Marie Hundhausen:** conceptualization; writing – review and editing; visualisation; formal analysis; methodology. **Annabell Weber:** writing – review and editing; visualisation; formal analysis; methodology. **Regina Kohlhepp:** writing – review and editing; formal analysis; methodology. **Christine Mihalyfi-Dean:** writing – review and editing; methodology. **Janus W. Schipper:** writing – review and editing; methodology. **Hendrik Feldmann:** conceptualization; writing – review and editing; methodology; funding acquisition.

Acknowledgements

We thank Hans-Jürgen Panitz (KIT/IMKTRO) for his help in the COSMO-CLM simulations. The simulations were performed on the national supercomputers Cray XC40 Hazel Hen and HPE Apollo Hawk at the High Performance Computing Center Stuttgart (HLRS) under the grant number HRCM/12801. Data processing and analysis were performed at the German Climate Computing Center (DKRZ). We thank the German Weather Service (Deutscher Wetterdienst, DWD) for providing the HYRAS data, and the Met Office Hadley Centre/Climatic Research Unit for the HadCRUT5 dataset. We also thank two anonymous reviewers for their helpful and constructive comments. Open Access funding enabled and organized by Projekt DEAL.

Funding

German Federal Ministry of Research, Technology and Space (BMFTR) projects RegIKlim-ISAP (01LR2007B, 01LR2007B1) and RegIKlim-NUKLEUS (01LR2002B, 01LR2002B1); German Federal Ministry

for the Environment, Climate Action, Nature Conservation and Nuclear Safety (BMUKN) project LandWandel (67DAS235A); AXA Research Fund.

Conflicts of Interest

The authors declare no conflicts of interest.

Data Availability Statement

The KIT-KLIWA simulation data are available on request from the authors. The HYRAS dataset is available from the German Weather Service, and the HadCRUTS dataset from the Met Office Hadley Center/Climate Research Unit.

Endnotes

[1]www.kliwa.de.

[2]www.regiklim.de, www.project.uni-stuttgart.de/isap.

[3]www.dwd.de/DE/service/lexikon/Functions/glossar.html.

References

Alexander, L., and N. Herold. 2016. Climpact2: Indices and Software. https://climpact-sci.org/assets/climpact2-user-guide.pdf.

Alexander, L. V., X. Zhang, T. C. Peterson, et al. 2006. "Global Observed Changes in Daily Climate Extremes of Temperature and Precipitation." *Journal of Geophysical Research: Atmospheres* 111: D05109. https://doi.org/10.1029/2005JD006290.

Alfieri, L., B. Bisselink, F. Dottori, et al. 2017. "Global Projections of River Flood Risk in a Warmer World." *Earth's Future* 5: 171–182. https://doi.org/10.1002/2016EF000485.

Baldauf, M., A. Seifert, J. Förstner, D. Majewski, M. Raschendorfer, and T. Reinhardt. 2011. "Operational Convective-Scale Numerical Weather Prediction With the COSMO Model: Description and Sensitivities." *Monthly Weather Review* 139: 3887–3905. https://doi.org/10.1175/MWR-D-10-05013.1.

Ban, N., C. Caillaud, E. Coppola, et al. 2021. "The First Multi-Model Ensemble of Regional Climate Simulations at Kilometer-Scale Resolution, Part I: Evaluation of Precipitation." *Climate Dynamics* 57: 275–302. https://doi.org/10.1007/s00382-021-05708-w.

Barriopedro, D., E. M. Fischer, J. Luterbacher, R. M. Trigo, and R. García-Herrera. 2011. "The Hot Summer of 2010: Redrawing the Temperature Record Map of Europe." *Science* 332: 220–224. https://doi.org/10.1126/science.1201224.

Benjamini, Y., and Y. Hochberg. 1995. "Controlling the False Discovery Rate: A Practical and Powerful Approach to Multiple Testing." *Journal of the Royal Statistical Society. Series B, Statistical Methodology* 57: 289–300. http://www.jstor.org/stable/2346101.

BfN. 2015. *Shapefiles of the Major Landscapes*. Federal Agency for Nature Conservation. https://www.bfn.de/en/topic/maps-and-data.

Biesbroek, G. R., R. J. Swart, T. R. Carter, et al. 2010. "Europe Adapts to Climate Change: Comparing National Adaptation Strategies." *Global Environmental Change* 20: 440–450. https://doi.org/10.1016/j.gloenvcha.2010.03.005.

Bordoni, S., S. M. Kang, T. A. Shaw, I. R. Simpson, and L. Zanna. 2025. "The Futures of Climate Modeling." *npj Climate and Atmospheric Science* 8: 99. https://doi.org/10.1038/s41612-025-00955-8.

Buontempo, C., H. M. Hanlon, M. Bruno Soares, et al. 2018. "What Have We Learnt From EUPORIAS Climate Service Prototypes?" *Climate Services* 9: 21–32. https://doi.org/10.1016/j.cliser.2017.06.003.

Buontempo, C., R. Hutjes, P. Beavis, et al. 2020. "Fostering the Development of Climate Services Through Copernicus Climate Change Service (C3S) for Agriculture Applications." *Weather and Climate Extremes* 27: 100226. https://doi.org/10.1016/j.wace.2019.100226.

Cannon, A. J., S. R. Sobie, and T. Q. Murdock. 2015. "Bias Correction of GCM Precipitation by Quantile Mapping: How Well Do Methods Preserve Changes in Quantiles and Extremes?" *Journal of Climate* 28: 6938–6959. https://doi.org/10.1175/JCLI-D-14-00754.1.

Cole, R., S. Hajat, P. Murage, et al. 2023. "The Contribution of Demographic Changes to Future Heat-Related Health Burdens Under Climate Change Scenarios." *Environment International* 173: 107836. https://doi.org/10.1016/j.envint.2023.107836.

Collins, W., N. Bellouin, M. Doutriaux-Boucher, et al. 2011. "Development and Evaluation of an Earth-System Model–hadgem2." *Geoscientific Model Development* 4: 1051–1075. https://doi.org/10.5194/gmd-4-1051-2011.

Corfee-Morlot, J., I. Cochran, S. Hallegatte, and P.-J. Teasdale. 2011. "Multilevel Risk Governance and Urban Adaptation Policy." *Climatic Change* 104: 169–197. https://doi.org/10.1007/s10584-010-9980-9.

Da Silva, N. A., and J. O. Haerter. 2025. "Super-Clausius–Clapeyron Scaling of Extreme Precipitation Explained by Shift From Stratiform to Convective Rain Type." *Nature Geoscience* 18: 382–388. https://doi.org/10.1038/s41561-025-01686-4.

Frich, P., L. V. Alexander, P. Della-Marta, et al. 2002. "Observed Coherent Changes in Climatic Extremes During 2nd Half of the 20th Century." *Climate Research* 19: 193–212. https://doi.org/10.3354/cr019193.

Fünfgeld, H., D. Fila, and H. Dahlmann. 2023. "Upscaling Climate Change Adaptation in Small- and Medium-Sized Municipalities: Current Barriers and Future Potentials." *Current Opinion in Environmental Sustainability* 61: 101263. https://doi.org/10.1016/j.cosust.2023.101263.

Giorgetta, M. A., J. Jungclaus, C. H. Reick, et al. 2013. "Climate and Carbon Cycle Changes From 1850 to 2100 in MPI-ESM Simulations for the Coupled Model Intercomparison Project Phase 5." *Journal of Advances in Modeling Earth Systems* 5: 572–597. https://doi.org/10.1002/jame.20038.

Hackenbruch, J., T. Kunz-Plapp, S. Müller, and J. Schipper. 2017. "Tailoring Climate Parameters to Information Needs for Local Adaptation to Climate Change." *Climate* 5: 25. https://doi.org/10.3390/cli5020025.

Hackenbruch, J., G. Schädler, and J. W. Schipper. 2016. "Added Value of High-Resolution Regional Climate Simulations for Regional Impact Studies." *Meteorologische Zeitschrift* 25: 291–304. https://doi.org/10.1127/metz/2016/0701.

Hasel, K., M. Buegelmayer-Blaschek, and H. Formayer. 2023. "A Statistical Approach on Estimations of Climate Change Indices by Monthly Instead of Daily Data." *Atmosphere* 14: 1634. https://doi.org/10.3390/atmos14111634.

Huang, H., H. Cui, and Q. Ge. 2021. "Assessment of Potential Risks Induced by Increasing Extreme Precipitation Under Climate Change." *Natural Hazards* 108: 2059–2079. https://doi.org/10.1007/s11069-021-04768-9.

Hundhausen, M., H. Feldmann, R. Kohlhepp, and J. G. Pinto. 2024. "Climate Change Signals of Extreme Precipitation Return Levels for Germany in a Transient Convection-Permitting Simulation Ensemble." *International Journal of Climatology* 44: 1454–1471. https://doi.org/10.1002/joc.8393.

Hundhausen, M., H. Feldmann, N. Laube, and J. G. Pinto. 2023. "Future Heat Extremes and Impacts in a Convection-Permitting Climate Ensemble Over Germany." *Natural Hazards and Earth System Sciences* 23: 2873–2893. https://doi.org/10.5194/nhess-23-2873-2023.

Hundhausen, M., H. J. Fowler, H. Feldmann, and J. G. Pinto. 2025. "Sub-Hourly Precipitation and Rainstorm Event Profiles in a Convection-Permitting Multi-GCM Ensemble." *Weather and Climate Extremes* 48: 100764. https://doi.org/10.1016/j.wace.2025.100764.

IPCC. 2007. *Climate Change 2007: Synthesis Report. Contribution of Working Groups I, II and III to the Fourth Assessment Report of the Intergovernmental Panel on Climate Change (Technical Report)*, edited by Core Writing Team, R. K. Pachauri, and A. Reisinger, 104. IPCC. https://www.ipcc.ch/site/assets/uploads/2018/02/ar4_syr_full_report.pdf.

IPCC. 2023. *Climate Change 2021: The Physical Science Basis. Contribution of Working Group I to the Sixth Assessment Report of the Intergovernmental Panel on Climate Change*. Cambridge University Press. https://doi.org/10.1017/9781009157896.

Jacob, D., J. Petersen, B. Eggert, et al. 2014. "EURO-CORDEX: New High-Resolution Climate Change Projections for European Impact Research." *Regional Environmental Change* 14: 563–578. https://doi.org/10.1007/s10113-013-0499-2.

Jendritzky, G., R. de Dear, and G. Havenith. 2011. "UTCI—Why Another Thermal Index?" *International Journal of Biometeorology* 56: 421–428. https://doi.org/10.1007/s00484-011-0513-7.

Kendon, E. J., E. M. Fischer, and C. J. Short. 2023. "Variability Conceals Emerging Trend in 100yr Projections of UK Local Hourly Rainfall Extremes." *Nature Communications* 14: 1133. https://doi.org/10.1038/s41467-023-36499-9.

Krinner, G., and M. G. Flanner. 2018. "Striking Stationarity of Large-Scale Climate Model Bias Patterns Under Strong Climate Change." *Proceedings of the National Academy of Sciences* 115: 9462–9466. https://doi.org/10.1073/pnas.1807912115.

Kunz-Plapp, T., J. Hackenbruch, and J. W. Schipper. 2016. "Factors of Subjective Heat Stress of Urban Citizens in Contexts of Everyday Life." *Natural Hazards and Earth System Sciences* 16: 977–994. https://doi.org/10.5194/nhess-16-977-2016.

Lee, T. M., E. M. Markowitz, P. D. Howe, C.-Y. Ko, and A. A. Leiserowitz. 2015. "Predictors of Public Climate Change Awareness and Risk Perception Around the World." *Nature Climate Change* 5: 1014–1020. https://doi.org/10.1038/nclimate2728.

Lehmann, P., M. Brenck, O. Gebhardt, S. Schaller, and E. Süßbauer. 2015. "Barriers and Opportunities for Urban Adaptation Planning: Analytical Framework and Evidence From Cities in Latin America and Germany." *Mitigation and Adaptation Strategies for Global Change* 20: 75–97. https://doi.org/10.1007/s11027-013-9480-0.

Lemos, M. C., C. J. Kirchhoff, and V. Ramprasad. 2012. "Narrowing the Climate Information Usability Gap." *Nature Climate Change* 2: 789–794. https://doi.org/10.1038/nclimate1614.

Lucas-Picher, P., D. Argüeso, E. Brisson, et al. 2021. "Convection-Permitting Modeling With Regional Climate Models: Latest Developments and Next Steps." *WIREs Climate Change* 12: e731. https://doi.org/10.1002/wcc.731.

Ludwig, P., F. Ehmele, M. J. Franca, et al. 2023. "A Multi-Disciplinary Analysis of the Exceptional Flood Event of July 2021 in Central Europe – Part 2: Historical Context and Relation to Climate Change." *Natural Hazards and Earth System Sciences* 23: 1287–1311. https://doi.org/10.5194/nhess-23-1287-2023.

Mann, H. B., and D. R. Whitney. 1947. "On a Test of Whether One of Two Random Variables Is Stochastically Larger Than the Other." *Annals of Mathematical Statistics* 18: 50–60. http://www.jstor.org/stable/2236101.

Maraun, D. 2016. "Bias Correcting Climate Change Simulations – A Critical Review." *Current Climate Change Reports* 2: 211–220. https://doi.org/10.1007/s40641-016-0050-x.

Measham, T. G., B. L. Preston, T. F. Smith, et al. 2011. "Adapting to Climate Change Through Local Municipal Planning: Barriers and Challenges." *Mitigation and Adaptation Strategies for Global Change* 16: 889–909. https://doi.org/10.1007/s11027-011-9301-2.

Moemken, J., H. Feldmann, J. G. Pinto, et al. 2021. "The Regional Miklip Decadal Prediction System for Europe: Hindcast Skill for Extremes and User-Oriented Variables." *International Journal of Climatology* 41: E1944–E1958. https://doi.org/10.1002/joc.6824.

Mohr, S., U. Ehret, M. Kunz, et al. 2023. "A Multi-Disciplinary Analysis of the Exceptional Flood Event of July 2021 in Central Europe – Part 1: Event Description and Analysis." *Natural Hazards and Earth System Sciences* 23: 525–551. https://doi.org/10.5194/nhess-23-525-2023.

Mora, C., B. Dousset, I. R. Caldwell, et al. 2017. "Global Risk of Deadly Heat." *Nature Climate Change* 7: 501–506. https://doi.org/10.1038/nclimate3322.

Morice, C. P., J. J. Kennedy, N. A. Rayner, et al. 2021. "An Updated Assessment of Near-Surface Temperature Change From 1850: The HadCRUT5 Data Set." *Journal of Geophysical Research: Atmospheres* 126: e2019JD032361. https://doi.org/10.1029/2019JD032361.

Nijsse, F. J., P. M. Cox, and M. S. Williamson. 2020. "Emergent Constraints on Transient Climate Response (TCR) and Equilibrium Climate Sensitivity (ECS) From Historical Warming in CMIP5 and CMIP6 Models." *Earth System Dynamics* 11: 737–750. https://doi.org/10.5194/esd-11-737-2020.

Papalexiou, S. M., and A. Montanari. 2019. "Global and Regional Increase of Precipitation Extremes Under Global Warming." *Water Resources Research* 55: 4901–4914. https://doi.org/10.1029/2018WR024067.

Pichelli, E., E. Coppola, S. Sobolowski, et al. 2021. "The First Multi-Model Ensemble of Regional Climate Simulations at Kilometer-Scale Resolution Part 2: Historical and Future Simulations of Precipitation." *Climate Dynamics* 56: 3581–3602. https://doi.org/10.1007/s00382-021-05657-4.

Prein, A. F., W. Langhans, G. Fosser, et al. 2015. "A Review on Regional Convection-Permitting Climate Modeling: Demonstrations, Prospects, and Challenges." *Reviews of Geophysics* 53: 323–361. https://doi.org/10.1002/2014RG000475.

Prodhomme, C., F. Doblas-Reyes, O. Bellprat, and E. Dutra. 2016. "Impact of Land-Surface Initialization on Sub-Seasonal to Seasonal Forecasts Over Europe." *Climate Dynamics* 47: 919–935. https://doi.org/10.1007/s00382-015-2879-4.

Randall, D. A., C. M. Bitz, G. Danabasoglu, et al. 2019. "100 Years of Earth System Model Development." *Meteorological Monographs* 59: 12.1–12.66. https://doi.org/10.1175/AMSMONOGRAPHS-D-18-0018.1.

Rauthe, M., H. Steiner, U. Riediger, A. Mazurkiewicz, and A. Gratzki. 2013. "A Central European Precipitation Climatology – Part I: Generation and Validation of a High-Resolution Gridded Daily Data Set (HYRAS)." *Meteorologische Zeitschrift* 22: 235–256. https://doi.org/10.1127/0941-2948/2013/0436.

Razafimaharo, C., S. Krähenmann, S. Höpp, M. Rauthe, and T. Deutschländer. 2020. "New High-Resolution Gridded Dataset of Daily Mean, Minimum, and Maximum Temperature and Relative Humidity for Central Europe (HYRAS)." *Theoretical and Applied Climatology* 142: 1531–1553. https://doi.org/10.1007/s00704-020-03388-w.

Rockel, B., A. Will, and A. Hense. 2008. "The Regional Climate Model COSMO-CLM (CCLM)." *Meteorologische Zeitschrift* 17: 347–348. https://doi.org/10.1127/0941-2948/2008/0309.

Schär, C., and G. Jendritzky. 2004. "Hot News From Summer 2003." *Nature* 432: 559–560. https://doi.org/10.1038/432559a.

Schipper, H., J. Hackenbruch, H. Lentink, K.-U. Nerding, and S. Müller. 2016. Sensitivitätsbereiche von Branchenspezifischen Klimakenngrößen in Baden-Württemberg – die "Sensitivitätsampel". Tech Rep, Karlsruhe. https://www.lubw.baden-wuerttemberg.de/klimawandel-und-anpassung/projektbeschreibung-klimopass/-/asset_publisher/YgFNnlWGQXn3/content/sensitivitatsbereiche-von-branchenspezifischen-klimakenngro-en-in-baden-wurttemberg.

Schipper, J., J. Hackenbruch, H. Lentink, and K. Sedlmeier. 2019. "Integrating Adaptation Expertise Into Regional Climate Data Analyses

Through Tailored Climate Parameters." *Meteorologische Zeitschrift* 28: 41–57. https://doi.org/10.1127/metz/2019/0878.

Schuldt, B., A. Buras, M. Arend, et al. 2020. "A First Assessment of the Impact of the Extreme 2018 Summer Drought on Central European Forests." *Basic and Applied Ecology* 45: 86–103. https://doi.org/10.1016/j.baae.2020.04.003.

Schwertfeger, B. T., G. Lohmann, and H. Lipskoch. 2023. "Introduction of the BiasAdjustCXX Command-Line Tool for the Application of Fast and Efficient Bias Corrections in Climatic Research." *SoftwareX* 22: 101379. https://doi.org/10.1016/j.softx.2023.101379.

Ssymank, A. 1994. "Neue Anforderungen im Europäischen Naturschutz: das Schutzgebietssystem Natura 2000 und die FFH-Richtlinie der EU." *Natur Und Landschaft* 69: 395–406. https://orlis.difu.de/handle/difu/19243.

Taylor, K. E., R. J. Stouffer, and G. A. Meehl. 2012. "An Overview of CMIP5 and the Experiment Design." *Bulletin of the American Meteorological Society* 93: 485–498. https://doi.org/10.1175/BAMS-D-11-00094.1.

Teichmann, C., K. Bülow, J. Otto, et al. 2018. "Avoiding Extremes: Benefits of Staying Below +1.5°C Compared to +2.0°C and +3.0°C Global Warming." *Atmosphere* 9: 115. https://doi.org/10.3390/atmos9040115.

Tiedtke, M. 1989. "A Comprehensive Mass Flux Scheme for Cumulus Parameterization in Large-Scale Models." *Monthly Weather Review* 117: 1779–1800. https://doi.org/10.1175/1520-0493(1989)117<1779:ACMFSF>2.0.CO;2.

Tölle, M. H., L. Schefczyk, and O. Gutjahr. 2018. "Scale Dependency of Regional Climate Modeling of Current and Future Climate Extremes in Germany." *Theoretical and Applied Climatology* 134: 829–848. https://doi.org/10.1007/s00704-017-2303-6.

Umweltbundesamt. 2024. Kommunalbefragung Klimaanpassung 2023. Tech. Rep. 34/2024. https://www.umweltbundesamt.de/sites/default/files/medien/11850/publikationen/34_2024_cc_kommunalbefragung.pdf.

Van Engelen, A., A. Klein Tank, G. van der Schrier, and L. Klok. 2008. *European Climate Assessment & Dataset (ECA&D), Report 2008. Tech Rep.* De Bilt. https://www.ecad.eu//documents/ECAD_report_2008.pdf.

Vautard, R. 1990. "Multiple Weather Regimes Over the North Atlantic: Analysis of Precursors and Successors." *Monthly Weather Review* 118: 2056–2081. https://journals.ametsoc.org/view/journals/mwre/118/10/1520-0493_1990_118_2056_mwrotn_2_0_co_2.xml.

Vautard, R., A. Gobiet, S. Sobolowski, et al. 2014. "The European Climate Under a 2°C Global Warming." *Environmental Research Letters* 9: 34006. https://doi.org/10.1088/1748-9326/9/3/034006.

VDI. 2012. *VDI Guideline 2067: Economic Efficiency of Building Installations – Fundamentals and Economic Calculation*. Verein Deutscher Ingenieure e.V. https://www.vdi.de/en/home/vdi-standards/details/vdi-2067-blatt-1-economic-efficiency-of-building-installations-fundamentals-and-economic-calculation.

Venäläinen, A., and M. Kangas. 2003. "Estimation of Winter Road Maintenance Costs Using Climate Data." *Meteorological Applications* 10: 69–73. https://doi.org/10.1017/S1350482703005073.

Vogel, J., M. Kolian, A. St Juliana, et al. 2020. "Past Is Prologue: A Case Study Exploration of the Role of Climate Indicators in Adaptation in the United States." *Climate Services* 20: 100202. https://doi.org/10.1016/j.cliser.2020.100202.

Voldoire, A., E. Sanchez-Gomez, D. Salas y Mélia, et al. 2013. "The CNRM-CM5. 1 Global Climate Model: Description and Basic Evaluation." *Climate Dynamics* 40: 2091–2121. https://doi.org/10.1007/s00382-011-1259-y.

Wallace, J. M., and D. S. Gutzler. 1981. "Teleconnections in the Geopotential Height Field During the Northern Hemisphere Winter." *Monthly Weather Review* 109: 784–812. https://journals.ametsoc.org/view/journals/mwre/109/4/1520-0493_1981_109_0784_titghf_2_0_co_2.xml.

Wanner, H., S. Brönnimann, C. Casty, et al. 2001. "North Atlantic Oscillation – Concepts and Studies." *Surveys in Geophysics* 22: 321–381. https://doi.org/10.1023/A:1014217317898.

Wilcoxon, F. 1945. "Individual Comparisons by Ranking Methods." *Biometrics Bulletin* 1: 80–83. http://www.jstor.org/stable/3001968.

Wilks, D. S. 2016. ""The Stippling Shows Statistically Significant Grid Points": How Research Results Are Routinely Overstated and Overinterpreted, and What to Do About It." *Bulletin of the American Meteorological Society* 97: 2263–2273. https://journals.ametsoc.org/view/journals/bams/97/12/bams-d-15-00267.1.xml.

Wilks, D. 2020. *Statistical Methods in the Atmospheric Sciences*. 4th ed. Elsevier. https://doi.org/10.1016/C2017-0-03921-6.

Winsemius, H. C., J. Aerts, L. Van Beek, et al. 2016. "Global Drivers of Future River Flood Risk." *Nature Climate Change* 6: 381–385. https://doi.org/10.1038/nclimate2893.

Zhang, X., L. Alexander, G. C. Hegerl, et al. 2011. "Indices for Monitoring Changes in Extremes Based on Daily Temperature and Precipitation Data." *WIREs Climate Change* 2: 851–870. https://doi.org/10.1002/wcc.147.

Zubler, E. M., S. C. Scherrer, M. Croci-Maspoli, M. A. Liniger, and C. Appenzeller. 2014. "Key Climate Indices in Switzerland; Expected Changes in a Future Climate." *Climatic Change* 123: 255–271. https://doi.org/10.1007/s10584-013-1041-8.

Supporting Information

Additional supporting information can be found online in the Supporting Information section. **APPENDIX S1:** Supporting information. **APPENDIX S2:** Supporting information.